



MINISTRY OF AVIATION

AERONAUTICAL RESEARCH COUNCIL

CURRENT PAPERS

Temperature Measurements on a Plasma Jet

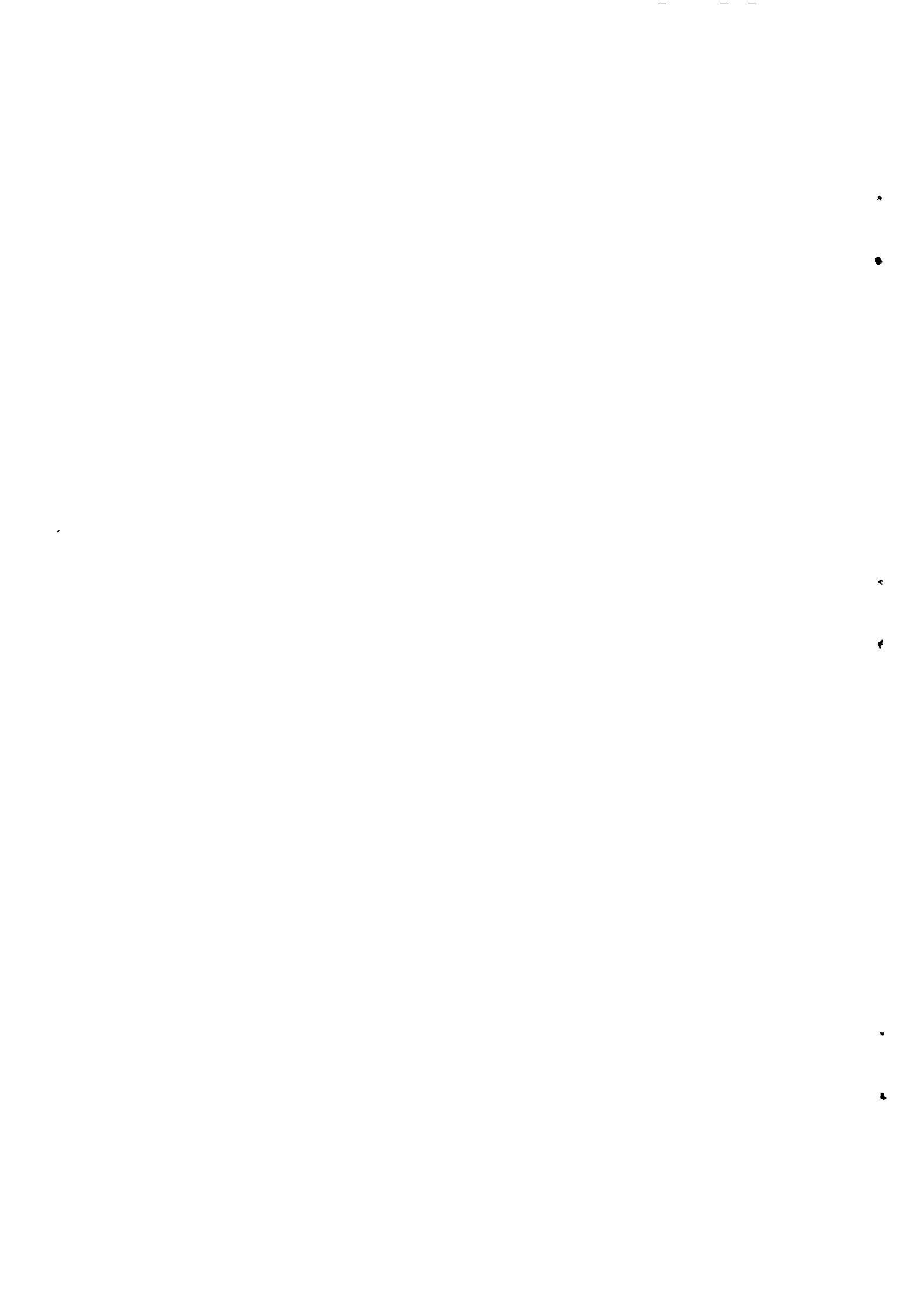
by

A. Wells and R. H. Kennett

LONDON: HER MAJESTY'S STATIONERY OFFICE

1964

TEN SHILLINGS NET



February 1964

TEMPERATURE MEASUREMENTS ON A PLASMA JET

by

A. Wells
(Aero Department)

and

R. H. Kennett
(W.R.E. Salisbury S Australia, attached
to Space Department, R.A.E.,
April 1962 - April 1963)

SUMMARY

Temperature measurements have been performed using spectroscopic techniques on the plasma jet obtained from a water stabilized arc with carbon electrodes.

The jet spectrum in the visible region consisted primarily of band spectra of molecular CN and C₂ and the Stark-broadened atomic line spectra of hydrogen. Intensities in various parts of these spectra were measured and temperatures were then deduced

- (a) from unresolved rotation line intensities in the CN 0-1 band,
- (b) from unresolved band intensities in the CN and C₂ systems,
- (c) from total intensities in the hydrogen H β and H γ lines,
- (d) from the stark-broadened line profiles of the H β and H γ lines,

Temperatures were also measured by the method of spectrum-line reversal on the C₂ 1-0 band head.

Temperatures obtained simultaneously from measurements on the CN band systems and the H β line profiles differed considerably; an average temperature of 5800°K \pm 300°K was obtained from measurements on the CN band spectrum whilst a temperature of 10,960°K \pm 400°K was obtained from the H β profile. This apparent inconsistency has been attributed to the existence of zones at different temperatures in the jet structure.

Observed jet instabilities have been reported and discussed and the limitations of the experimental techniques have also been commented upon.

CONTENTS

	<u>Page</u>
NOMENCLATURE	5
1 INTRODUCTION	6
2 TEMPERATURE MEASUREMENTS ON MOLECULAR SPECTRA OF CN AND C ₂	8
2.1 Discussion of the methods of measurement	8
2.1.1 Resolved rotation-lines in CN bands	9
(i) Rotation-line intensities	9
(ii) Intersection wave number	9
2.1.2 CN or C ₂ bands with unresolved rotational structure	10
(i) Top-height ratio	12
(ii) Integrated first band	12
2.1.3 Line-reversal observations on the C ₂ 1-0 band	13
2.2 Experimental details	14
2.2.1 Photographic spectroscopy	14
2.2.2 Plate calibration	14
2.2.3 Other measurements	15
2.3 Results	15
2.3.1 CN band spectra	16
2.3.2 C ₂ band spectra	17
2.4 Comments on the results from molecular spectra	18
3 TEMPERATURE AND ELECTRON DENSITY MEASUREMENTS ON SPECTRAL LINES OF ATOMIC HYDROGEN IN THE BALMER SERIES	18
3.1 Discussion of the methods of measurement	18
3.1.1 Spectrum-line intensity ratios of H β and H γ	18
3.1.2 Spectrum-line intensity distributions of H β and H γ	19
3.2 Experimental details	20
3.3 Results	21
3.3.1 Spectrum-line intensities of H β and H γ	21
3.3.2 Intensity distributions in H β and H γ	22
3.4 Comments on the results from atomic hydrogen spectra	23

CONTENTS (Contd)

	<u>Page</u>
4 GENERAL DISCUSSION OF RESULTS	23
4.1 Comparison of temperatures from hydrogen spectra with temperatures from molecular spectra	23
4.2 Effects of jet instabilities	25
5 CONCLUDING REMARKS	26
ACKNOWLEDGEMENTS	27
REFERENCES	28
APPENDICES 1 - 3	30-37
ILLUSTRATIONS - Figs. 1 - 10	-
DETACHABLE ABSTRACT CARDS	-

APPENDICES

Appendix

1 Summary of theory of temperature measurement using band spectra	30
2 Values of Franck Condon factors	33
3 Calculation of plasma temperature from measured values of electron density	34

ILLUSTRATIONS

	<u>Fig.</u>
Plasma jet apparatus together with a high-speed cine film record of the plasma jet	1
Jet spectrum for a range of arc conditions	2
Interdependence of spectral characteristics of the plasma jet on the arc voltage, current and length	3
Spectrogram and microdensitometer trace of $B^2\Sigma^+ - X^2\Sigma^+$ CN 0-1 band	4
Theoretical intensity profile and experimental microdensitometer trace of CN 0-1 and CN 1-2 unresolved band spectra	5
Dependence on temperature of top-height intensity ratio and integrated first band intensities	6

ILLUSTRATIONS (Contd)

	<u>Fig.</u>
Time-resolved intensity variations in the plasma jet	7
Theoretical and experimental intensity distributions in the H β line (4861 Å) of hydrogen	8
Theoretical and experimental intensity distributions in the H γ line (4340 Å) of hydrogen	9
Dependence of water plasma temperature on contamination with carbon	10

NOMENCLATURE

b	spectrograph slit function (cm^{-1})
c	velocity of light ($2.998 \times 10^{10} \text{ cm sec}^{-1}$)
e	electronic charge (1.602×10^{-19} coulomb) (4.802×10^{-10} e. s. u.)
g	statistical weight
h	Planck's constant (6.625×10^{-34} joule sec)
k	Boltzmann's constant (1.380×10^{-23} joule $^{\circ}\text{K}^{-1}$)
m	electronic mass (9.108×10^{-31} Kgm)
v	vibrational quantum number
x	degree of carbon contamination
A	transition probability (sec^{-1})
\AA	wavelength in Angstrom units (10^{-8} cm)
B(T)	partition function
B_v	$\left\{ \begin{array}{l} \text{rotational constants of diatomic molecules } (\text{cm}^{-1}) \end{array} \right.$
D_v	
E	energy (joules; eV; cm^{-1})
$F(v', v'')$	Franck - Condon factor
$I(\bar{\nu})$	intensity of a spectrum line of wave number ($\bar{\nu}$) (watts cm^{-2} ster $^{-1}$ cm)
$J(\bar{\nu})$	intensity measured at wave number, ($\bar{\nu}$), in unresolved band profile (watts cm^{-2} ster $^{-1}$ cm)
J	rotation quantum number
N	particle number density (cm^{-3})
S	rotation line strength
T	temperature ($^{\circ}\text{K}$)
A	$\left\{ \begin{array}{l} \text{Notation of electronic energy states in diatomic molecules} \end{array} \right.$
B	
X	

NOMENCLATURE (Contd)

Σ	{ designation of states in diatomic molecules according to their angular momenta
Π	
ψ	Saha function
χ	ionization potential (eV)
$\bar{\nu}$	wavenumber (cm^{-1})

Subscripts

e	electrons
i	ions
el	electronic
rot	rotational
vib	vibrational
C	carbon
H	hydrogen
O	oxygen
P	{ designation of branches in rotational structure
Q	
R	

Superscripts

'	upper energy state
''	lower energy state
+	ion

1 INTRODUCTION

This paper summarises the results of attempts to measure, by optical means, the temperature of the jet of hot gas (plasma jet) produced by a water stabilized arc with carbon electrodes. The apparatus and cine photographs of the plasma jet are shown in Fig.1. This type of plasma jet, first devised by Weiss¹, has been used in R.A.E. for experimental studies on hot gases and preliminary estimates of the jet temperature were made using the method of spectrum-line

reversal on the sodium D-lines². Results obtained from these estimates indicated temperatures of about 4500°K to 5500°K which were much less than the temperatures of 9000°K to 13,000°K previously reported by Weiss.

The objects of the present work have been to investigate possible causes for these differences, to examine the practicability of applying a variety of optical methods of temperature measurement to sources of radiating gas (e.g. plasma jets, arc discharges or shock-heated gases) and to relate the measured temperatures to the physical processes at work in the plasma jet. All the optical methods described depend upon some feature of the spectral distribution of the energy radiated by the hot gas. The kind of spectrum emitted depends upon the chemical constituents in the gas and on the state of excitation of each of the constituents. One expects the plasma jet to contain matter originating from the water vapour in the arc channel, carbon and traces of impurities from the electrodes, and air constituents which become entrained in the jet. The spectrum of the jet could, therefore, consist of molecular, atomic or ionic spectra of any of these constituents together with the spectrum of any of their products of chemical reaction. In the visible and near ultra-violet regions, the spectra of a variety of such constituents were indeed detected, namely

- (a) the band spectrum of the CN radical,
- (b) the band spectrum of diatomic carbon, C₂, (Swan bands),
- (c) the atomic hydrogen spectrum in the Balmer series,
- (d) atomic lines of oxygen and electrode impurities.

The types of radiating species and the intensities of their spectra were both found to vary with the manner in which the arc was operated. These effects are illustrated in typical spectrograms, Fig. 2, and shown diagrammatically in Fig. 3

In this work it has been assumed that although temperature gradients exist in the jet, any small volume of radiating gas will be in a state of thermal equilibrium and therefore a unique temperature can be attributed to it. Theoretical justification of this assumption of thermal equilibrium in plasmas at atmospheric pressure is to be found in the literature³ and in the case of the ordinary low-current carbon arc experimental evidence of thermal equilibrium has also been reported⁴.

In a volume of gas in thermal equilibrium, the intensity of the radiation depends upon the equilibrium temperature. Relationships between radiation and temperature which are based upon well-established theoretical foundations⁵ have been invoked to deduce the jet temperature from various features of the spectra of CN, C₂ or atomic hydrogen. In this work, jet temperatures have been evaluated from measurements of

- (a) intensities of rotation lines in the B²Σ⁺ - X²Σ⁺ CN 0-1 band,
- (b) intensities of unresolved band profiles of CN- and C₂-band systems,
- (c) ratios of total intensities of the hydrogen Hβ and Hγ lines,
- (d) intensity profiles of the hydrogen Hβ and Hγ lines,

Temperatures have also been measured by the application of the method of spectrum-line reversal on the $A^3\Pi_g - X^3\Pi_u$ C_2 1-0 band using a high temperature background source.

Attempts have been made, wherever possible, to measure the jet temperature by the simultaneous application of at least two different methods so that the results could be compared.

It has been found convenient in what follows to allocate complete sections first to the theory and measurements applicable to the molecular spectra of CN and C_2 , and secondly to the theory and measurements applicable to the atomic hydrogen spectrum in the Balmer series.

2 TEMPERATURE MEASUREMENTS ON MOLECULAR BAND SPECTRA OF CN AND C_2

The strengths of emission of the spectra of CN and C_2 in the plasma jet were related to the arc operating conditions in the manner illustrated in Figs. 2 and 3.

Temperature measurements based upon these spectra mostly involved measuring the intensities of either resolved rotation lines or unresolved vibration-rotation bands in the electronic spectra of the molecules and comparing the measured intensities with theoretical intensities of molecular systems in thermal equilibrium calculated for a range of given temperatures. These methods, which are summarised in the following sections, are only applicable in conditions in which self-absorption in the relevant part of the spectrum is negligibly small. As Fig. 3 shows, in certain ranges of arc current and voltage, self-absorption in the CN bands was not negligible. In those regions of the arc characteristics where self-absorption in both the CN and C_2 bands was sufficiently strong temperatures could be estimated by an entirely different method, the method of visual spectrum-line reversal against a high-pressure xenon-discharge background source.

2.1 Discussion of the methods of measurement

The major part of the experimental work was concerned with deducing jet temperatures from intensity measurements of the band spectra of CN or C_2 . A brief account of the theory of the intensities of molecular spectra has been extracted from the comprehensive treatment by G. Herzberg⁵ and included in Appendix 1 of this note.

Four distinct methods of temperature measurement of differing sensitivity and all based on the theory in Appendix 1 were applied to the jet and these can be subdivided into two groups. In Section 2.1.1 below, those methods are discussed which depend upon intensity measurements on partially-resolved rotational spectra in the band structure; in Section 2.1.2 the methods discussed depend upon measurements of intensity distributions in unresolved band spectra.

Other temperature measurements by the method of spectrum-line reversal are described in Section 2.1.3. The experimental details and some additional experiments designed to investigate the spatial and temporal intensity variations throughout the jet structure are described in Section 2.2.

2.1.1 Resolved rotation-lines in CN-bands

The intensities of rotation lines in the CN-bands are related to the equilibrium temperature through equation 1 below (Ref. Appendix 1, equation 11)

$$\begin{aligned} I(P) &= \text{Constant } (\bar{\nu}_P)^4 J_P'' \exp(-E'_{\text{rot}}/kT) \\ I(R) &= \text{Constant } (\bar{\nu}_R)^4 (J_R'' + 1) \exp(-E'_{\text{rot}}/kT) \end{aligned} \quad (1)$$

Spectrograms taken with a 30,000 lines/inch grating spectrograph (5 Å/mm dispersion at 4200 Å) showed that much of the rotation line structure in the $B^2\Sigma^+ - X^2\Sigma^+$ CN 0-1 band could be resolved and consequently identified (e.g. Figs. 4a and 4b). As the total line intensity of each resolved line was found to be proportional to its peak intensity, it was not necessary to take any account of the effects of line width and line profile on rotation-line intensities. Temperatures were deduced from spectrograms such as Fig. 4a by two methods:-

(i) Rotation-line intensities

Intensities of resolved rotation lines were measured and the quantities $I(P)/(\bar{\nu}_P)^4 J_P''$ and $I(R)/(\bar{\nu}_R)^4 (J_R'' + 1)$ calculated: the slope of a graphical plot of $\log_e I(P)/(\bar{\nu}_P)^4 J_P''$ and $\log_e I(R)/(\bar{\nu}_R)^4 (J_R'' + 1)$ against E'_{rot} was evaluated and the temperature was calculated from this slope which is equal to $1/kT$ by equation 1.

Because of inherent inaccuracies in the processes of photographic photometry, rotation-line intensities could not be measured to better than $\pm 6\%$; the corresponding uncertainty in temperature was $\pm 200^\circ\text{K}$.

A further source of error in measured temperatures would exist if self-absorption were present in the resolved rotation lines, causing their intensities to be underestimated. Self-absorption increases with increasing line intensity in the band with corresponding increase in the discrepancy between the measured line intensity and the line intensity with negligible self-absorption. Rotation line intensity, self-absorption and consequently the error in measured line intensity all reach a maximum in the line $J_P'' = 30$ for a temperature of 5800°K . The effect of self-absorption would be detected by non-linearity of the plot of $\log_e I(P)/(\bar{\nu}_P)^4 J_P''$ against E'_{rot} , although the linearity of such a graph would also be disturbed by any steep temperature gradients existing in regions of the jet containing radiating CN. Systematic errors in the measured temperatures due to self-absorption and/or temperature gradients were estimated from curvature of the graphical plots of $\log_e I(P)/(\bar{\nu}_P)^4 J_P''$ against E'_{rot} and found to be $\pm 400^\circ\text{K}$.

(ii) Intersection wave-number

The temperature dependence of the intersection wave-number of the P- and R-branch intensity profiles in the CN 0-1 band has been used by Greenshields⁶

to determine gas temperatures from CN spectra. From equation 1, theoretical rotation-line intensities can be calculated for any chosen temperature, and intensities of lines in the P- and R-branches plotted against the wave-numbers of the lines. The wave-number at which the intensity profiles of the two branches intersect is dependent only upon the chosen temperature. A curve relating the variation of intersection wave-number to the temperature then provides the means of determining the temperature of gas containing radiating CN from resolved rotation-line spectra (see Ref.6).

This method has several advantages over the previous method. The intersection wave-number can be obtained directly from optical density measurements on the spectrogram (e.g. Fig.4b) so that calibration of the emulsion can be avoided. Some self-absorption in the spectral lines can be tolerated since near the branch profile intersection, lines of nearly equal intensity and therefore nearly equal self-absorption are compared (at nearly equal wave-numbers).

The method is most applicable for temperatures between 3700°K and 5500°K. Above 5500°K, the intersection wave-number of the P- and R-branches falls within the region of the unresolved CN 1-2 band as Fig.4b shows; its value can be obtained only approximately by extrapolation of the branch profiles into this unresolved region and the process becomes increasingly inaccurate at higher temperatures. The method cannot be used for temperatures in excess of 6200°K.

Random errors in temperature arising from emulsion grain effects and the possible presence of interfering radiation limit the accuracy of the method to $\pm 200^{\circ}\text{K}$ for temperatures below 5500°K; above this temperature errors may rise to $\pm 600^{\circ}\text{K}$.

The effects of spin splitting of rotation lines in the P-branch with large values of J_p'' has also been considered as a possible source of error. However, in CN, the doublet separation of these lines⁷ was only about one-third of the measured half-width of the lines. Therefore, it is unlikely that the peak intensities of the P-branch lines were greatly affected by spin splitting and the effects on the intersection wave-number have been taken as negligible.

In both the methods described above, the line intensities depend upon the distribution of molecules among the rotation states of a single vibration energy level. The temperature subsequently deduced would then be a rotation temperature if complete thermal equilibrium did not exist in the radiating gas.

2.1.2 CN- or C₂-bands with unresolved rotational structure

Even when the rotation-line structure of a band spectrum is not resolved by the spectrograph, certain features of the intensity profiles of the unresolved band can be related to the temperature of the radiating gas. Comparisons between theoretical and experimental intensity profiles of unresolved CN-bands were first used for temperature measurement by Smit-Miessen and Spier⁸ and Spier and Smit⁷ who computed their theoretical intensity profiles from equations of the form 10 (a, c). (Ref. Appendix 1 equation 10).

For this present work, theoretical profiles were computed in greater detail than the Smit-Miessen profiles using the Mercury computer. First, profiles for bands in the $B^2\Sigma^+ - X^2\Sigma^+$ CN systems, which only contain P- and R-branches in their rotational structures, were computed and then profiles for bands in the $A^3\Pi_g - X^3\Pi_u$ C_2 system containing P-, Q- and R-branches were computed.

The following paragraph is a summary of the machine programme for computing intensity profiles.

Wave-numbers of the first 75 lines of each branch were calculated by substituting into equation 8, Appendix 1, all relevant spectroscopic data for $\bar{\nu}_0$, B'_v and B''_v obtained from Herzberg⁵ and Pearse and Gaydon⁹. The intensity of each line relative to the reference line $J''_P = 1$ in the first band was then calculated from equation 2 (Appendix 1, equation 10).

P-branch

$$I_{\text{rel}}(P) = \left(\frac{\bar{\nu}_P}{\bar{\nu}_0}\right)^4 \frac{F(v', v'')}{F(m, n)} S(P) \exp - \frac{hc}{kT} \left\{ \epsilon(v', 0) - \epsilon(m, 0) + B'_v(J'' - 1) J'' - D'_v (J'' - 1)^2 J''^2 \right\} \quad (2a)$$

Q-branch

$$I_{\text{rel}}(Q) = \left(\frac{\bar{\nu}_Q}{\bar{\nu}_0}\right)^4 \frac{F(v', v'')}{F(m, n)} S(Q) \exp - \frac{hc}{kT} \left\{ \epsilon(v', 0) - \epsilon(m, 0) + B'_v(J'' + 1) J'' - D'_v (J'' + 1)^2 J''^2 \right\} \quad (2b)$$

R-branch

$$I_{\text{rel}}(R) = \left(\frac{\bar{\nu}_R}{\bar{\nu}_0}\right)^4 \frac{F(v', v'')}{F(m, n)} S(R) \exp - \frac{hc}{kT} \left\{ \epsilon(v', 0) - \epsilon(m, 0) + B'_v(J'' + 1)(J'' + 2) - D'_v (J'' + 1)^2 (J'' + 2)^2 \right\} \quad (2c)$$

The Franck-Condon factors, $F(v', v'')$ were the average values taken from all available literature. (See Appendix 2). In earlier programmes, a rectangular slit function, 'b', was assumed ('b' is the width in cm^{-1} in the image plane of

the spectrograph that the image of the slit would assume if the slit were illuminated with purely monochromatic radiation). The computer was required to calculate and print out at intervals of wave-number $\Delta\bar{\nu} = 0.5 \text{ cm}^{-1}$ the intensity of the unresolved profile, $J(\bar{\nu})$ at the wave-number $\bar{\nu}$.

For a rectangular slit function

$$J(\bar{\nu}) = \frac{1}{b} \int_{\bar{\nu}-b/2}^{\bar{\nu}+b/2} I_{(\text{PQR})}(\bar{\nu}) d\bar{\nu} \quad (3)$$

where $I_{(\text{PQR})}(\bar{\nu})$ are the intensities of all lines lying in the wave-number range $\bar{\nu} - \frac{b}{2} \leq \bar{\nu} \leq \bar{\nu} + \frac{b}{2}$. This calculation was repeated at intervals,

$\Delta\bar{\nu} = 0.5 \text{ cm}^{-1}$ throughout the whole wave-number range covered by the bands under consideration. In a later programme*, the profiles were re-computed using a triangular slit function which is a crude approximation to the various bell-shaped distributions found in actual spectral lines. The intensity $J(\bar{\nu})$ of the unresolved profile at wave-number, $\bar{\nu}$, for a triangular slit function and spectrum-line half width, 'b', is given by

$$J(\bar{\nu}) = \frac{1}{b} \int_{\bar{\nu}-b}^{\bar{\nu}+b} (b - |\bar{\nu}_{(\text{PQR})} - \bar{\nu}|) I_{(\text{PQR})}(\bar{\nu}) d\bar{\nu} \quad (4)$$

The rectangular slit function represents a situation in which the spectrograph entrance slit width is large compared with the true half-width of a spectrum line; the use of a triangular slit function approximates to a situation where either the slit function is determined primarily by diffraction phenomena, or the rotation lines in the band spectrum are broadened due to physical processes (Doppler, collision or statistical broadening). The choice of slit function only seriously affects the profiles when the choice of 'b' corresponds to a situation in which the rotation line structure is almost resolved.

A number of profiles were calculated for different temperatures and slit functions, 'b', and the theoretical dependence on temperature of the two following intensity ratios were evaluated.

- (i) The ratio of band-head intensities of the first two bands in a sequence (top-height ratio method).
- (ii) The ratio of the integrated first-band intensity to the product of the band tail intensity and the band head separation (cm^{-1}). (Integrated first-band method).

* The later programme was written by the second author for the IBM 7094 computer at the Lincoln Laboratories, M.I.T.

These ratios which are illustrated in Fig. 5 were chosen since they show the minimum dependence on the choice of entrance-slit width, 'b'.

Temperatures were deduced from experimental profiles by evaluating the above ratios and comparing them with the theoretical ratios shown in Fig. 6.

All intensity measurements were considered to be limited by an uncertainty of at least $\pm 6\%$ with a corresponding uncertainty in temperature of $\pm 600^\circ\text{K}$ by the top-height ratio method, (i), and an uncertainty of $\pm 1000^\circ\text{K}$ by the integrated first-band method (ii). Uncertainties in the Franck-Condon factors contribute to a further uncertainty in temperatures obtained by method (i) of $\pm 200^\circ\text{K}$.

Self-absorption is again a potential source of error but its effects have tended to cancel out in much of the work using the top-height ratio method because, at the measured temperatures, the heads of the CN 1-2 and CN 0-1 bands consist of rotation lines of almost equal intensities. This situation does not exist, however, in either the CN 1-1/CN 0-0 or C_2 1-1/ C_2 0-0 band heads so that the presence of self-absorption would cause temperatures obtained from these spectra to be overestimated.

Self-absorption, however, seriously affects the total band-intensity profile so that temperatures deduced by the integrated first-band method (ii) are susceptible to its effects. Preferential self-absorption occurs near the band head where the rotation-line intensities are greatest so that the temperature tends to be overestimated. In this work, as is shown later, self-absorption in the CN 0-1 band is sufficiently strong for the temperature to be overestimated by several thousand degrees Kelvin.

Whereas in method (ii) the intensity distribution in the first band in a sequence depends only upon rotation-energy states, therefore giving a rotation temperature in non-equilibrium conditions, in method (i) the band-head intensity ratio depends upon the relative populations of the first two vibration states in the excited electronic state of the molecule. In non-equilibrium conditions therefore method (i) would give a temperature which would be, primarily, a vibration temperature.

2.1.3 Line-reversal observations on the unresolved C_2 1-0 band

Visual line-reversal observations on the C_2 1-0 band head were performed under conditions in which the constituent spectral lines in these spectra were so strongly self-absorbing that the conditions applying to equations 1 and 2 were completely violated.

The C_2 1-0 band was chosen for this measurement as the wavelength of the band head corresponds to the wavelength region ($4700 \text{ \AA} - 4750 \text{ \AA}$) in which the brightness temperature of the xenon lamp is a maximum¹⁰.

An image of the discharge in the high-pressure xenon lamp was focused in the plane of the plasma jet and the relevant part of the jet spectrum was viewed against the background of the continuum spectrum of the xenon lamp. The brightness temperature of the xenon lamp was adjusted, through variation of the lamp current until the matched condition was attained, and the C_2 band head could not be distinguished either in emission or absorption against the background

continuum. The jet temperature was then taken to be equal to the brightness temperature of the xenon lamp. The brightness temperature of the lamp was measured by the method described in detail in reference 10.

2.2 Experimental details

2.2.1 Photographic spectroscopy

Resolved rotation-band spectra were photographed using a grating spectrograph which had a plane reflection grating in the Littrow mount and a linear dispersion of 5 Å/mm at 4200 Å: unresolved band profiles were obtained using a Hilger Medium Glass Prism Spectrograph with a linear dispersion of 15 Å/mm at 4200 Å.

The intensities of the molecular spectra were measured using the methods of photographic photometry on spectrograph plates. The variations of optical density (with wavelength) on the spectrum plates were measured with a Joyce Loebel Recording Microdensitometer Mk. III. Figs. 4 and 5 include typical records. Intensities were subsequently evaluated from these microdensitometer records through calibration of the photographic emulsion of each plate used for the measurements, and temperatures were evaluated from the intensity data using the methods indicated in Section 2.1.

2.2.2 Plate calibration

Each plate was calibrated by measurement of the characteristic curve (i.e. the variation of optical density with incident intensity) at any chosen wavelength, and the spectral response (i.e. the variation of density with wavelength for constant incident spectral energy flux) in the required wavelength regions.

In most of the earlier work with the Hilger Medium Glass Spectrograph, the plates were calibrated solely in terms of the spectral radiant energy distribution of a Philips tungsten-ribbon-filament standard lamp. A number of exposures was made extending over a range of time intervals and the standard lamp, maintained at constant intensity, was used as the source of radiation. These exposures were placed on adjacent regions of the plate. After the plate had been developed, optical densities corresponding to these various calibrating spectra were measured with the microdensitometer and characteristic curves of density against total exposure (intensity X exposure time) were plotted at the chosen wavelengths.

The optical density in an emulsion obeying the reciprocity law would remain constant for constant total exposure. However, in an emulsion exhibiting reciprocity failure, the density corresponding to constant total exposure depends upon the exposure time.

Where the ratio of exposure times of tungsten lamp and jet respectively was not greater than 30:1 for the Ilford N30 plates used in these measurements, the contribution to the total error in intensity due to reciprocity failure was not greater than 6%, but under conditions in which the intensities of spectrum lines in the jet exceeded the spectral intensity of the tungsten lamp by two or more orders of magnitude, reciprocity failure in the emulsion caused large errors and the above method of calibration was discarded. Instead,

calibration was performed with an iron-arc source in which the spectrum-line intensities were comparable with line intensities in the jet.

The spectrograph slit was uniformly illuminated with radiation from the iron arc, a calibrated Rhodium-on-Quartz step-wedge filter was placed at the slit and the spectrum of the iron arc was photographed through the full length of the slit. Relative intensities of radiation emerging from different parts of the slit were therefore known, the corresponding densities on the plates were measured with the microdensitometer and a characteristic curve of density against relative intensity was plotted in the required wavelength region by judicious selection of suitable iron lines for measurement. A single spectrum of the tungsten lamp was also included on the plate so that changes in spectral sensitivity of the emulsion over moderate wavelength ranges could also be measured.

From the characteristic curves, prepared by either method, relative intensities of details within the band spectra were evaluated and the accuracy of the intensity measurements was also estimated.

2.2.3 Other measurements

In a separate experiment, the jet spectrum from a complete horizontal section of the vertical jet was photographed and analysed.

Time-resolved intensity measurements within the CN O-1 vibration band were made using a Hilger constant-deviation spectroscope which had a photomultiplier detector mounted at the exit slit and a typical record of one such measurement is shown in Fig.7.

High-speed ciné film records (e.g., Fig.1) were also taken which showed spatial and temporal fluctuations in luminosity in the jet in the spectral region $4000 \text{ \AA} - 4600 \text{ \AA}$ defined by a suitable filter.

2.3 Results

All the results discussed below are summarized in Table 1.

TABLE 1

Summary of plasma jet temperatures from molecular spectra

Method of measurement		Jet temperature °K			
Arc condition Voltage V Current I		140V 220A	90V 260A	70V 285A	40V 310A
Rotation line intensities CN 0-1	Section 2.1.1(i)		6400°K ±200°K		
Intersection wave-number CN 0-1	Section 2.1.1(ii)		5790°K ± 80°K		
Top-height ratio CN 1-2/CN 0-1	Section 2.1.2(i)		5940°K ±170°K	6700°K ±600°K	
Top-height ratio CN 1-1/CN 0-0	Section 2.1.2(i)	5350°K	5970°K ±260°K		
Top-height ratio C ₂ 1-1/C ₂ 0-0	Section 2.1.2(i)		6400°K ±200°K		
Integrated first band CN 0-1	Section 2.1.2(ii)		10550°K ±240°K	7800°K	
Integrated first band CN 0-0	Section 2.1.2(ii)	8000°K	6400°K ±800°K		
Spectrum-line reversal C ₂ 1-0 band head	Section 2.1.3				5450°K ±250°K

2.3.1 CN-band spectra

The jet temperature has been evaluated from intensity measurements on bands in the violet CN system at 4216 Å and 3883 Å by the methods described in Sections 2.1.1 and 2.1.2. These measurements were taken at a fixed height of 0.7 cm above the cathode and looking through the centre of the jet under the standardized arc running conditions (see Table 1). Where quoted temperatures are the average values of several measurements, the mean temperatures and standard deviations have been calculated.

Measurements by the Rotation Line Intensities method in the CN 0-1 band were made on spectrograms taken with the grating spectrograph. Errors in intensity due to reciprocity failure had been minimised and intensities were measurable to within ±6% so that self-absorption was the major source contributing to errors in the measured temperatures.

The temperatures obtained by the Intersection-Wave-Number method are considered to be more reliable because the need to calibrate the emulsion has been avoided and because the method is insensitive to the effects of self-absorption.

All intensity measurements on unresolved CN-bands were made on spectrograms taken with the Hilger Medium Glass Spectrograph. Measurements on CN 1-2 and CN 0-1 bands using the top-height ratio method were not greatly affected by reciprocity failure and, as has been discussed previously, self-absorption in the lines in each of the band heads was of comparable intensity. Therefore, provided that the degree of self-absorption was small, though not necessarily negligible, the major source of error originated from the emulsion calibration procedure and intensities were considered to be measurable to within $\pm 6\%$. Intensity measurements on the CN 1-1 and CN 0-0 bands were more susceptible to the effects of self-absorption but these results were, in any case, considered to be less reliable than the CN 1-2/CN 0-1 results through difficulties with the emulsion calibration. This calibration was much less dependable than in all other measurements because, owing to the low specific intensity of the tungsten lamp at the wavelengths 3883 \AA and 3871 \AA (CN 0-0 and CN 1-1 band heads) the calibrating exposures to the tungsten lamp were always considerably longer than the jet exposures, with correspondingly larger errors due to reciprocity failure.

Temperatures obtained by the Integrated-First-Band method could be in error due to the effects of self-absorption and emulsion calibration errors, and the temperatures are almost certainly over-estimated, for this reason.

Self-absorption in the CN-bands appeared to be small (less than 20%) when the jet was delivered from the 90V - 260A arc yet its effects were in evidence in results obtained from the Rotation-Line-Intensities and Integrated-First-Band methods. With other arc conditions (70V - 285A; 40V - 310A) self-absorption was much greater and none of the methods could strictly be applied since they are all derived from a theory assuming an optically thin medium.

2.3 2 C₂-band spectrum

Not many reliable measurements have been made using the C₂-band spectrum. For the 90V and 140V arc conditions, the C₂-bands were generally too weak (relative to the CN-bands) for intensity measurements to be made simultaneously on both systems; for the 70V and 40V arc conditions, self-absorption appeared to be too strong in the C₂-bands for reliable measurement. The one available result from the C₂ 1-1/C₂ 0-0 bands using the top-height ratio method is subject to possible errors due to self-absorption, the effects of which do not cancel out in this case. The temperature may thus be overestimated.

The jet obtained from the 40V - 310A arc was very strongly self-absorbing in the CN- and C₂-bands and visual line-reversal observations were possible on the C₂ 1-0 band head. Temperature measurements by this method were subject to the errors in the calibration of the xenon-lamp background source already discussed in Ref. 10.

2.4 Comments on the results from molecular spectra

It must be emphasised that all the above results of jet temperatures were obtained from intensity measurements which constituted an integrated value throughout the whole thickness of radiating plasma, for the duration of the exposure of the jet to the spectrograph plate. The time-resolved measurements (Fig.7) indicated large-amplitude, high-frequency, intensity fluctuations and further reduction of the data gave some evidence of steep temperature gradients within the jet (see Section 4). Generally, it is possible to deduce radial temperature distributions in an axially-symmetrical source from side-on intensity observations on a section of the source using the numerical solution of the Abel integral equation, (Edels, Hearne and Young¹¹). In the present case of the plasma jet, however, the information obtained from such a procedure would not be too meaningful. The apparently non-systematic intensity fluctuations shown in Fig.7, and the random variations in jet width as indicated by the high-speed cine film record of the jet, e.g. Fig.1, both demonstrate that this conventional Abel technique of analysis is not, applicable here. Therefore, although spatial temperature variations almost certainly exist in the jet, the quantitative nature of these variations is obscured by the large temporal variations occurring in the jet.

It is not altogether surprising, therefore, that there are discrepancies between the above results which are greater than one might expect in view of the estimated experimental errors. Associations between these discrepancies and the intensity fluctuations and other possible causes are discussed further in Section 4.

3 TEMPERATURE AND ELECTRON DENSITY MEASUREMENTS ON SPECTRAL LINES OF ATOMIC HYDROGEN IN THE BALMER SERIES

Spectrograms, which showed the H β (4861 Å) and H γ (4340 Å) lines in the Balmer series, (Fig.2) could be analysed to provide details of the total intensity of either of these lines together with their distribution of intensity against wavelength.

The manner in which jet temperatures are inferred from total line intensities depends upon underlying principles which are quite different to the principles on which the method of line-intensity distributions depends. For this reason the following section is divided to permit separate treatments of the two methods.

3.1 Discussion of the methods of measurement

3.1.1 Spectrum-line intensities of H β and H γ

The intensity of a spectrum line, in the absence of self-absorption, is related to the temperature of the radiating species through equation 5 provided that the radiating gas is in a state of thermal equilibrium.

$$I = \frac{hc\bar{\nu}\Lambda}{4\pi B(T)} N \exp(-E'/kT) \quad (5)$$

By comparing the relative intensities of the H β (4861 Å) and H γ (4340 Å) lines in the Balmer series, the excitation temperature was calculated from equation 6 which follows from equation 5.

$$\log_{10}(I/g'A\bar{\nu})_{H\beta} - \log_{10}(I/g'A\bar{\nu})_{H\gamma} = \frac{0.6217}{T} (E'_{H\gamma} - E'_{H\beta}) \quad (6)$$

The values of transition probability, A, statistical weight, g', energy level, E', and wave-number, $\bar{\nu}$, for the hydrogen atom were obtained from astrophysical tables¹² and the total relative intensities of the H β and H γ lines were measured, either photographically or, for the purposes of time-resolved temperature measurement, photoelectrically. Total line intensities were measured from spectrum plates in terms of spectral intensity over the wavelength range of the broadened lines, the area under the best average curve through plots of experimental spectral intensities against wavelength being proportional to total line intensity. Each measured spectral intensity could only be determined to within $\pm 6\%$ because of the limitations of the emulsion calibration procedure. If both total line intensities of H β and H γ lines were determined to this accuracy, there would be a corresponding uncertainty in temperature of $\pm 1680^{\circ}\text{K}$, but this uncertainty may be overestimated since the process of fitting the best average curve through the experimental points tends to average out random errors in spectral intensity arising from the emulsion calibration procedure.

As the spectral response of the Ilford N30 emulsion had been calibrated and found to be fairly uniform over the wavelength range 4100 Å to 4900 Å errors arising from the calibration of the wavelength sensitivity of the emulsion were considered to be negligibly small.

By using photoelectric rather than photographic means of detection, one has, in principle, eliminated a major source of error from the measurement of temperature but in the time-resolved photoelectric measurements of total intensity described in Section 3.2 though the deflection sensitivity and estimated calibration error of the photoelectric detection system permitted total intensity ratios to be measured to within $\pm 5\%$, the corresponding uncertainty in temperature was still $\pm 1400^{\circ}\text{K}$.

Systematic errors in measurement of total line intensity could have arisen from the presence of disturbing background spectra; if such background radiation affected the H γ rather than the H β line then the temperature would be overestimated by 280°K per 1% error in intensity at the actual measured temperatures.

Errors due to self-absorption were negligible in the H β and H γ lines which were found to be optically thin at the measured temperatures.

3.1.2 Spectrum-line intensity distributions of H β and H γ

The H β and H γ spectrum lines found in the plasma are broadened because of the perturbation, through the Stark effect, of the energy levels of the radiating atoms by the local electric field arising from the presence of the ions and electrons.

Recently, the intensity - wavelength distributions of hydrogen lines have been calculated (by Griem, Kolb and Shen¹³) from theoretical considerations which take into account the effects of electron-atom collisions superimposed upon the Stark-effect splitting of the multiplet energy states of emitting atoms in the presence of the electric fields of the more slowly moving ions. The theoretical intensity profile depends mainly on the electron density (N_e) and the total ion density (N^+) so that provided plasma conditions prevail, ($N_e = N^+$) comparison of an experimentally-derived intensity profile with the appropriate theoretical profile can be made to yield a measurement of electron density.

Plasma temperatures have been deduced from the measured values of electron density using the type of calculation described in a paper by Pusey, Lapworth and Metherell¹⁴. In the present work, the calculation has been made more general in order to account for the effects of contamination with electrode carbon in the hydrogen-oxygen plasma since this case is more appropriate to measurements on the plasma jet. A detailed account of this extended treatment is given in Appendix 3.

Since the spectral intensities and therefore the experimental line profiles could only be measured to within $\pm 6\%$, the electron density, N_e , deduced from comparison of the experimental and theoretical profiles, similarly, could only be determined to within $\pm 6\%$. However as the theoretical profile could only be computed to an accuracy of $\pm 20\%$ (Ref. 13) the uncertainty in measurement of the experimental profile due to emulsion calibration would not greatly affect the accuracy of the determination of electron density. On the other hand, systematic errors in the determination of N_e would be experienced if any disturbing background spectrum existed and had not been allowed for.

The electron density is a sensitive function of temperature and uncertainties in the measurement of electron density of $\pm 20\%$ lead to uncertainties in temperature of $\pm 3\%$. Far greater errors may exist in the calculated temperatures because the chemical constitution of the plasma could not be specified. Further discussion of this source of error has been included in Section 3.3.2.

3.2 Experimental details

The hydrogen spectrum was photographed with the Hilger Medium Glass Spectrograph and the spectrum plates were analysed with the Joyce Loebel Recording Microdensitometer Mk III. Characteristic curves of the emulsion response were prepared for each plate by the methods described in Section 2.2, total intensities of the H β and H γ lines were measured and intensity profiles were constructed and compared with theoretical profiles. (See Appendix 3).

Time-resolved total line intensities of the whole broadened H β and H γ line emissions were also measured, separately and simultaneously with a pair of constant-deviation spectroscopes with photomultiplier detectors, one allocated to each "line". The intensities were recorded by photographing traces of the photomultiplier signals displayed on a dual-beam Tektronix 502 oscilloscope. In these measurements, temporal fluctuations up to 10 Kc/s could be detected. Each channel was subsequently calibrated - voltage against intensity - by a second measurement of the oscilloscope deflection corresponding

to the known intensity of a standard tungsten lamp, as measured through the same optical system.

3.3 Results

Temperatures given in Table 2 were measured at a fixed height of 0.7 cm above the cathode, looking through the centre of the jet under standardized arc running conditions. These results are discussed in the following sections.

TABLE 2

Typical plasma temperatures and electron densities
from atomic hydrogen spectra

Method of measurement	Arc V conditions I	140V 220A		90V 260A		70V 285A	
		$N_e \text{ cm}^{-3}$	T °K	$N_e \text{ cm}^{-3}$	T °K	$N_e \text{ cm}^{-3}$	T °K
H β profile (Plate A)	(Assuming no carbon contamination)	5.91×10^{16}	11850°K	5.27×10^{16}	11650°K	4.35×10^{16}	11350°K
H β profile (Plate B)	(Assuming no carbon contamination)			3.42×10^{16}	10950°K		
H γ (Blue wing) (Plate B)	(Assuming no carbon contamination)			2.96×10^{16}	10740°K		
Intensity ratio H β : H γ (Plate B)	Time-averaged (photographic detection)				10980°K		
Intensity ratio H β : H γ	Time-resolved (photoelectric detection)				9970°K ±660°K		

NOTE:

Experiments investigating the change in spectra with arc conditions produced results typified by those from Plate A. Results on H γ were not often obtained from these experiments. Plate B was one of the few results on which analysis of the H γ line was possible.

3.3.1 Spectrum-line intensities of H β and H γ

Temperatures obtained from the time-averaged line-intensity ratios of the H β and H γ lines were subject to the usual emulsion calibration error. Since the temperature is sensitive to small changes in intensity ratio, an uncertainty in the intensity measurements due to emulsion calibration of ±6% leads to uncertainties in temperature of up to ±1680°K. Errors due to the presence of interfering background spectra were also in evidence. In the red wing of the H γ

line, 4340 Å - 4390 Å, spectra of the C₂ (Swan) 2-0, 3-1, 4-2 bands were frequently detected. For example, in the quoted results using measurements on Plate B, the intensity of the C₂ radiation contributed about 5% to the total measured intensity in the region of the H_γ line and an approximate correction was made to the value of the H_γ intensity before the temperature was computed. In the majority of measurements taken on the H_β and H_γ profiles, the contribution of the C₂ background radiation was so great that temperatures could not be calculated with any confidence.

Time-resolved temperatures were subject to an uncertainty of ±1400°K, through uncertainties in calibration of the photoelectric detection system. Again, this is a manifestation of the sensitivity of the line-intensity ratio method to errors in the measured intensity ratio. The time-resolved results are also susceptible to the effects of interfering spectra. Thus a further uncertainty is added to the temperature values.

3.3.2 Intensity distributions of H_β and H_γ lines

Theoretical and experimental intensity distributions in the H_β and H_γ lines taken from Plate B are shown in Figs. 8 and 9 respectively. The particular electron densities calculated from these profiles are also shown on the figures and in Table 2. The poor agreement between theoretical and experimental intensities in the line wings of both lines is undoubtedly due to the fact that intensities in the line wings were measured making use of the insensitive "toe" of the emulsion characteristic curve. Errors in intensity arising through inaccurate calibration of the emulsion in this region could be consistently greater than the average value of 6% and, consequently, the line wings have been largely ignored in determining the best fit between experimental and theoretical line profiles.

The overall fit between theoretical and experimental H_γ profiles is seen, in Fig. 9, to be inferior to that obtained with the H_β profiles, particularly in the case of the red wing, 4340 Å - 4390 Å, for which the experimental intensities are greater than the theoretical intensities. This effect is due to the interference of the background spectrum of the C₂ (Swan) 2-0, 3-1, 4-2 bands. Although the magnitude of this contribution to the total measured intensity in the region of the H_γ line has been estimated to be less than 5% of the total intensity, the H_γ profile cannot be corrected precisely enough in order to obtain a better fit between theoretical and experimental profiles. Therefore, only results of electron density obtained from the blue wings of the H_γ line have been included although even these may not be completely free from the effects of background intensity of disturbing spectra.

The H_β line appears to be relatively free from background spectra and, except in the far line wings, measured intensities agree with theoretical intensities to well within the ±20% accuracy claimed for the theoretical profile by Griem, Kolb and Shen¹³.

The electron densities, N_e, obtained from the H_β and H_γ (blue wing) using the results from Plate B were:- N_e = 3.42 × 10¹⁶ cm⁻³ from the H_β profile and N_e = 2.96 × 10¹⁶ cm⁻³ from the H_γ profile (blue wing). The latter value of N_e is considered to be consistent with the value obtained from the H_β profile within the limits of the anticipated accuracy of the method.

Plasma temperatures have been calculated from the measured values of electron density according to the method outlined in Appendix 3. Ideally, the calculation can only be performed if the exact composition of the plasma is known. Pusey, Lapworth and Metherell¹⁴ have performed the calculation assuming a pure water plasma. In this work, however, other sources of electrons arise from ionization of carbon and impurities from the electrodes and from the air entrained in the jet. As carbon was considered to be the major source of contamination at the higher plasma jet temperatures the calculation of plasma temperature has been extended, here, taking only the carbon contamination into account. The variation of temperature with degree of contamination has been calculated (Appendix 3) and this variation is shown in Fig. 10. (The degree of contamination is defined, here, as the number of carbon atoms per oxygen atom initially present in the constituents of the water plasma).

No reliable means has been found of measuring this contamination, directly, either in the jet or the arc, but the degree of contamination has been roughly estimated as follows. From Fig. 10 it can be seen that if the plasma is assumed to be uncontaminated with carbon, the calculated plasma temperature corresponding to $N_e = 3.42 \times 10^{16} \text{ cm}^{-3}$ was 10950°K (as shown in Table 2). The temperature obtained at the same time and under the same conditions from the ratio of total line intensities of $\text{H}\beta$ and $\text{H}\gamma$ (Section 3.3.1) was $10080^\circ\text{K} (\pm 1680^\circ\text{K})$. As the relative intensities of these lines are independent of the amount of carbon in the plasma, if the difference in temperature obtained by the two methods is assumed to be due only to carbon contamination, then reference to Fig. 10 shows that for the temperature difference of 870°K the degree of contamination would have to be of the order of 0.75. That is, there would be 0.75 carbon atoms per oxygen atom in the plasma.

3.4 Comments on the results from atomic hydrogen spectra

Whilst reasonably consistent values of electron density (N_e) and temperature were obtained from simultaneous measurements of $\text{H}\beta$ and $\text{H}\gamma$ intensity profiles, measurements of N_e from the $\text{H}\beta$ profile obtained from several spectrograms did not give reproducible values as a comparison of the results from Plates A and B in Table 2 indicates. This implies that the plasma was not reproducible either in form or temperature between one measurement and the next, and one must conclude that, in most of this work, inconsistencies arise as much from the instability of the jet as from lack of sensitivity of measuring technique. Since all the intensity measurements were integrated values throughout the whole thickness of the plasma, for the duration of the spectrum exposure times, all the effects of the measured intensity fluctuations also influence the interpretation of these results, but as the results from the molecular spectra are similarly affected a more detailed discussion of the effects of jet instability on all the results is deferred until Section 4.2.

4 GENERAL DISCUSSION OF RESULTS

4.1 Comparison of temperatures from hydrogen spectra with temperatures from molecular spectra

Tables 1 and 2 contain representative results of temperature measurements from both molecular and atomic spectra and demonstrate the large differences between temperatures obtained from the molecular spectra on the one hand and hydrogen spectra on the other for identical arc conditions. Discounting, for

the moment, the exceptions of the high temperatures obtained by the Integrated Band Profile method the other methods using molecular spectra all gave temperatures which are 4000°K to 5500°K below the temperatures obtained using the hydrogen spectra.

If this difference in temperature arises from the effects of temperature gradients in the jet, then the molecular species would be confined to the cooler regions whereas the atomic hydrogen would occur in the hot region of the jet. Some attempts have been made to obtain a quantitative description of the jet structure in order to determine the zonal distributions of the various species. In the separate experiments in which the jet spectrum of a complete horizontal section from the vertical jet was analysed, only radiation from the cooler molecular species was found to originate from outer peripheral regions in the jet - no atomic hydrogen could be detected in these regions. On the other hand, one cannot infer from the results obtained in these experiments whether the molecular species were present in significant quantities in the central regions of the jet, or not. However the results show quite definitely that atomic hydrogen existed only in the central regions.

Had the jet approximated to a stable, axially-symmetrical discharge, then measurements of spatial side-on intensity distributions could have been transformed into radial spatial-intensity distributions by numerical solution of the Abel integral equation¹¹; radial temperature distributions and consequently radial distributions of relative concentrations of the various radiating species could then have been deduced from the radial intensity distributions. However, because of the gross instabilities in the form of the plasma jet, any assumption that the jet was sufficiently stable and axially symmetrical for the Abel transformation to be applied could not be justified and for this reason no further analysis of the measured side-on intensity distributions was carried out.

Even though the experimental evidence for the existence of discrete zones of radiating molecular species and radiating atomic hydrogen is not conclusive, there are strong theoretical reasons for believing that these zones exist. Simple calculations using the dissociation equations (equation 4.21, Ref.15) of CN and C₂ show that in regions of high temperatures, very little CN or C₂ could exist, for these molecules would be almost completely dissociated. In the cooler peripheral regions, the degrees of dissociation would not be excessively high and these molecules could then exist in significant quantities. For example, the degree of dissociation of CN or C₂ molecules would be between two and three orders of magnitude greater at 10,000°K than at 6000°K, depending on the partial pressure of CN or C₂ in the plasma. A similar calculation using the excitation equation (equation 4.5, Ref.15) for the hydrogen atom shows that the degree of excitation in the excited states corresponding to the Balmer series is four orders of magnitude greater at 10,000°K than at 6000°K.

The complexity of the chemical constitution of the jet arises from the arc plasma, already containing an unknown quantity of carbon, being discharged into and reacting with atmospheric air in the characteristically unpredictable fashion of this jet. In spite of this complexity and although only order of magnitude calculations on the jet contents have been possible, the concept of temperature zones containing different radiating species seems to be supported by all the above results.

4.2 Effects of jet instabilities

The luminosity of the jet varied considerably during any single run, due to changes in the amount of carbon contamination in the jet. This in turn depended upon ablation rates at the anode and cathode, and the stability and variations in diameter of the water vortex channel all of these being features of the plasma jet apparatus which could not be controlled. Such factors as these presumably account for the lack of consistency between measurements taken at different times using the same method e.g. the differences in electron density obtained from H β profiles indicated in Table 2.

During any single measurement, of a few tenths of a second duration, the intensities were averaged over many cycles of apparently random, large magnitude intensity fluctuations of the type illustrated in Fig.7 and integrated over regions in the jet containing steep temperature gradients. The temperatures then deduced from these measurements could only be some indeterminate average value.

It has been suggested¹⁵ that temperatures calculated from the mean values of intensity (obtained from time-averaged measurement) could be almost as high as the temperatures corresponding to maximum intensities (obtained from time-resolved measurement) due to the exponential factor in equations 1 or 5. To test the applicability of this suggestion to the present results, the intensity waveform in Fig.7 which shows the peak-to-peak intensity fluctuations in the H β line to be $\pm 50\%$ about the mean intensity, has been substituted by a square waveform, maximum intensity $\frac{3I_m}{2}$, minimum value $\frac{I_m}{2}$ (I_m is the mean value of intensity). Using the method of comparison of intensities of H β and H γ the temperature obtained from the values of mean intensity I_m , is only 0.5% greater than the average temperature obtained by taking into account the square-wave fluctuations of intensity. This difference in temperature would be even smaller if the actual waveform in Fig.7 were used in the calculation. When a similar calculation was made on the rotation-line intensities of the CN 0-1 band the difference in temperature was 4%. Clearly in the case of the plasma jet, temperatures obtained from time-averaged intensity measurements do not differ greatly from actual mean temperatures averaged over a typical cycle of intensity fluctuation. However, the temperatures are still averaged over the temperature gradients in the jet because the jet structure cannot be resolved by the Abel transformation techniques in the usual way.

The possibilities of non-equilibrium conditions existing in the jet were also examined. An average temperature of 10,550^oK was evaluated with some degree of consistency using the Integrated First Band method and the unresolved intensity distributions in the CN 0-1 band obtained with the 90V - 260A arc. This temperature is clearly very different from all other temperatures obtained from molecular spectra. If the difference had been due to a departure from thermal equilibrium, one would have to submit that the CN molecules were not fully relaxed vibrationally even though vibration relaxation rates, at atmospheric pressure, are known to be very fast compared with the rates of emission of plasma from the arc into the jet. If non-equilibrium conditions did prevail, then the temperatures in question would be "rotation" temperatures whilst those obtained from the top-height ratios of the CN 1-2 and CN 0-1 bands would approximate to "vibration" temperatures. However, temperatures obtained from the Rotation-Line Intensities and Intersection Wave Number methods would also

be "rotation" temperatures in the event of non-equilibrium conditions prevailing in the jet. Since these latter results are seen to be more consistent with the "vibration" temperatures obtained by the top-height ratio method, the CN molecules in the jet were almost certainly fully relaxed and the high "rotation" temperatures measured by the Integrated First Band method are anomalous. From the above discussion, therefore, it is reasonable to conclude that conditions of thermal equilibrium prevailed in regions of the jet containing the radiating CN molecules and that the anomalous results were due to the strong self-absorption in the rotation lines in the CN 0-1 band structure.

5 CONCLUDING REMARKS

The existence in the plasma jet of at least two separate zones, one containing radiating CN and C₂ at temperatures around 6000°K and the other containing radiating atomic hydrogen at temperatures around 10,000°K is strongly indicated by all the measurements described in this paper. However, since no account has been taken of the effects of radial temperature gradients or the random intensity fluctuations in the jet, these measurements lack precision and consistency which might otherwise have been achieved. Apart from the anomalously high temperatures obtained by the Integrated First Band method, all other results are considered to be not inconsistent with one another within the limits of accuracy imposed by experimental errors in the intensity measurements, the existence of self-absorption in the molecular spectra, and the gross inhomogeneity of the plasma jet.

In considering the suitability of the various temperature measuring techniques for applications in other circumstances, it is unfortunate that this plasma jet has proved to be an unsuitable source with which to test these techniques to their ultimate limits. The main reasons for this were that the form of the plasma jet was always unstable and its chemical constitution could not be determined due to the unknown amounts of carbon contamination in the water-stabilized arc. Nevertheless, there are a number of conclusions which can be drawn concerning the use of the various methods. These are summarised below.

Of the methods applied to molecular spectra, those involving fully-resolved rotation spectra gave the more reproducible results. The Intersection Wave Number method is particularly attractive within its range of applicability (3700°K - 5800°K for CN 0-1) since calibration of the photographic emulsion is unnecessary and the method is insensitive to self-absorption. Hence the effects of two major sources of error can be minimised. However, the method is unsuitable for applications where spatial resolution is necessary and the temperature obtained by this method will always be averaged along the line of sight. Spatial resolution could be achieved with the Rotation-Line Intensity method provided that the geometrical form of the source was known and provided that self-absorption was negligible.

Similar criticisms apply to the Top-Height Ratio method but, because the lines in the band head are not resolved, it is often more difficult to decide from subsequent intensity measurements whether the criterion of optical thinness in the source has been satisfied. However, the method has the advantage over the Rotation-Line Intensities method that it measures an approximate vibration temperature in non-equilibrium conditions and that it could be adapted to high-

speed time resolution techniques using photoelectric detection. The Integrated First Band method suffers from all the disadvantages and few of the advantages of all the previous methods. The disadvantages of its sensitivity to self-absorption and interfering background radiation outweighs any advantage that its sensitivity to temperature changes might have. Yet this method might still provide the only means of deducing rotation temperatures in unresolved molecular spectra.

The usefulness of the Spectrum-Line Reversal method depends on the quality of the background source, and the xenon lamp used in this work has already been criticized in this role¹⁰. The temperature indicated by this method would always be averaged along the line of sight and would lie within the limits of the extremes of temperature in the source. Therefore, spatial resolution of temperature cannot be obtained by direct application of the method, which is best applied to temperature measurements on a uniform volume of radiating gas or a gas containing steep temperature gradients in which the radiating species under observation are highly localized.

The Line-Intensity Ratio method is adaptable either for spatial or temporal temperature resolution and could be adapted for simultaneous spatial and temporal resolution if enough channels for measurement could be made available. The application of the method to the hydrogen H β and H γ lines does not yield very accurate results because of the sensitivity of temperature to errors in the intensity ratio. The method is, therefore, very susceptible to the emulsion calibration errors and interfering background radiation.

In any radiating body of gas containing hydrogen, electron density can be reliably evaluated from the H β or H γ intensity profile provided that the profiles are unaffected by any interfering background spectrum. Spatial resolution of electron densities in a stable source could be achieved satisfactorily using measurements of the H β profile which is more sensitive than the H γ profile to changes in electron density. Subsequent accurate calculations of the equilibrium temperature using the measured electron-density values then depend upon detailed knowledge of the concentrations of the gas constituents.

The photographic emulsion has contributed to so many uncertainties in intensity measurements that, wherever possible, any future spectroscopy would be performed using photoelectric detection for intensity measurements. Under certain circumstances, however, e.g. studies of spectrum detail using short duration exposures the photoelectric detector is unsuitable and the photographic plate would still be necessary.

ACKNOWLEDGEMENTS

We are most grateful to Professor A. G. Gaydon of Imperial College, London for his advice and criticism in connection with this work and also wish to thank him for the loan of the grating spectrograph, the use of which enabled us to detect an anomalous result in the earlier work.

REFERENCES

- | <u>No.</u> | <u>Author</u> | <u>Title, etc.</u> |
|------------|--------------------------------------|--|
| 1 | Weiss, R. | Investigations on a plasma jet emitted from a high energy arc.
Z. für Physik Vol.138, 1954.
R.A.E. Translation 958. |
| 2 | Mitchell, A.H. | The temperature of a plasma jet as inferred from its emissive and absorptive powers.
Unpublished M.O.A. Report. |
| 3 | Finkelberg, W.
Maecker, H. | Electric arcs and thermal plasmas.
Handbuch der Physik, Vol.22 (1956) pp 309-315. |
| 4 | Smit, J.A. | The determination of temperature from spectra.
Physica Vol.XII, September 1946. |
| 5 | Herzberg, G. | Molecular spectra and molecular structure,
I Spectra of Diatomic Molecules, pp 204-207.
(Van Nostrand Co Inc. N.Y.) |
| 6 | Greenshields, D.H. | Spectrographic temperature measurements in a carbon-arc-powered air jet.
N.A.S.A. Tech Note D 169. December 1959. |
| 7 | Spier, J.L.
Smit, J.A. | Temperature determinations from the CN bands
4216 Å to 4197 Å.
Physica IX. July 1942. |
| 8 | Smit-Miessen, M.M.
Spier, J.L. | Intensity profiles of non-resolved CN bands.
Physica IX. February 1942. |
| 9 | Pearse, R.W.B.
Gaydon, A.G. | The identification of molecular spectra.
(Chapman and Hall). |
| 10 | Wells, A.A. | A study of a high pressure xenon discharge lamp as a background source for temperature measurements on a plasma jet by the line reversal method.
A.R.C. 24677. November 1962. |
| 11 | Edels, H.
Hearne, K.
Young, A. | Numerical solutions of the Abel integral equations.
Journal of Mathematics and Physics. March 1962. |
| 12 | Allen, C.W. | Astrophysical quantities.
(Athlone Press, 1962). |
| 13 | Griem, G
Kolb, A.
Shen, K. | Stark broadening of hydrogen lines in plasmas.
Phys Rev Vol.116 No.1, (1959).
N.R.L. Report 5455 Naval Research Labs.
Washington. P86353. |

REFERENCES (Contd)

- | <u>No.</u> | <u>Author</u> | <u>Title etc.</u> |
|------------|--|--|
| 14 | Pusey, P.
Lapworth, K.
Metherell, A. | Determination of ion density and temperature of a water-stabilised arc from observations of the line profiles of the hydrogen lines $H\beta$ and $H\gamma$.
A.R.C. C.P.614. June 1961. |
| 15 | Aller, L.H. | Astrophysics, the atmosphere of the sun and the stars.
pp 74-96.
Ronald Press Co. N.Y. (1953). |
| 16 | Halle, H.
Price, C.F. | Characterization and extension of simulation capabilities of the L.A.S. high temperature arc facility.
University of Chicago, Technical Document
ASD-TDR-62-463. |



APPENDIX 1

SUMMARY OF THEORY OF TEMPERATURE MEASUREMENT USING BAND SPECTRA

The nature of the spectra of diatomic molecules and the underlying theory are to be found in a most comprehensive treatment by G. Herzberg⁵. In the following paragraphs, the minimum theory necessary to establish the temperature dependence of the intensities of molecular spectrum lines has been extracted from Herzberg's treatment.

A whole band system such as the $B^2\Sigma^+ - X^2\Sigma^+$ CN violet system or the $A^3\Pi_g - X^3\Pi_u$ C_2 Swan system arises from a single electronic transition in the molecule. Any band in the system corresponds to a single transition between a pair of vibrational energy states and each line in a band corresponds to a single transition between a pair of rotational energy states.

The energy of any state in the molecular system is comprised of the energies of electronic, vibrational and rotational excitations.

$$E = E_{el} + E_{vib} + E_{rot} \quad (7)$$

The wavenumber of any rotation line in the system is given by

$$\begin{aligned} \bar{\nu} &= \frac{E' - E''}{hc} \\ &= \nu_0 + [B'_V J'(J' + 1) - D'_V J'^2(J' + 1)^2] \\ &\quad - [B''_V J''(J'' + 1) - D''_V J''^2(J'' + 1)^2] \end{aligned} \quad (8)$$

where the permitted transitions

$$\begin{array}{l} \Delta J = -1 \quad \text{P - Branch} \\ \Delta J = 0 \quad \text{Q - Branch} \\ \Delta J = +1 \quad \text{R - Branch} \end{array} \left\{ \begin{array}{l} \Delta J = J' - J'' \end{array} \right.$$

lead to the branch structure of rotation lines in a band. $\bar{\nu}_0$ has a unique value for each band in the system. The values of $\bar{\nu}_0$, B_V and D_V can be calculated from basic spectroscopic data given in Herzberg⁵ or Pearse and Gaydon⁹.

For a system in thermal equilibrium in which the energy states are populated according to the Maxwell-Boltzmann distribution, the absolute intensity of any rotational line is given by equation 9 below

$$I = \frac{hc \bar{\nu} A g' N}{4\pi B(T)} \exp - \frac{E'_{el} + E'_{vib} + E'_{rot}}{kT} \quad (9)$$

The intensity of any rotational line arising from the transition $(v', J') \rightarrow (v'', J'')$ relative to the line $J''_P = 1$ in the first band of the sequence $\Delta v = v' - v'' = \text{constant}$ is then given by equation 10 below. (Taking the first band in the sequence to correspond to the vibrational transition $v' = m \rightarrow v'' = n$).

P-branch

$$I_{rel}(P) = \left(\frac{\bar{\nu}_P}{\bar{\nu}_0} \right)^4 \frac{F(v', v'')}{F(m, n)} S(P) \exp - \frac{hc}{kT} \left\{ \epsilon(v', 0) - \epsilon(m, 0) + B'_v(J'' - 1)(J'') - D'_v(J'' - 1)^2(J'')^2 \right\} \quad (10a)$$

Q-branch

$$I_{rel}(Q) = \left(\frac{\bar{\nu}_Q}{\bar{\nu}_0} \right)^4 \frac{F(v', v'')}{F(m, n)} S(Q) \exp - \frac{hc}{kT} \left\{ \epsilon(v', 0) - \epsilon(m, 0) + B'_v(J'' + 1)(J'') - D'_v(J'' + 1)^2(J'')^2 \right\} \quad (10b)$$

R-branch

$$I_{rel}(R) = \left(\frac{\bar{\nu}_R}{\bar{\nu}_0} \right)^4 \frac{F(v', v'')}{F(m, n)} S(R) \exp - \frac{hc}{kT} \left\{ \epsilon(v', 0) - \epsilon(m, 0) + B'_v(J'' + 1)(J'' + 2) - D'_v(J'' + 1)^2(J'' + 2)^2 \right\} \quad (10c)$$

$F(v', v'')$ the Franck-Condon factor for the $v' \rightarrow v''$ transition, and $F(m, n)$ the Franck-Condon factor for the reference vibrational transition, are the vibration-dependent factors in the transition probabilities.

$S(P)$, $S(Q)$, $S(R)$, the rotational-line strengths for the appropriate branch given by the Hönl-London Formulae, equations IV-81 to IV-83 in Herzberg⁵ are the rotation dependent factors in the transition probabilities.

$\epsilon(v', 0)$ is the energy (in cm^{-1}) of the v' state above the $v'' = 0$ state.

In the case of the $B^2\Sigma^+ - X^2\Sigma^+$ CN band system, there are no Q-branches in the rotational structure and the relative line intensities in a single band can be represented by equation 11 below.

$$I(P) \propto \bar{\nu}_P^4 J_P'' \exp(-E_{\text{rot}}'/kT)$$
$$I(R) \propto \bar{\nu}_R^4 (J_R'' + 1) \exp(-E_{\text{rot}}'/kT) \quad (11)$$

The dependence of E_{rot}' on J'' has already been illustrated in equation 10.

APPENDIX 2

VALUES OF FRANCK-CONDON FACTORS

Ratios of Franck-Condon factors $F(v',v'')/F(m,n)$ for the CN $B^2\Sigma^+ - X^2\Sigma^+$ transitions and the C_2 (Swan) $A^3\Pi_g - X^3\Pi_u$ transitions were averaged values taken from the available literature.

For CN:

$$\frac{F(1,1)}{F(0,0)} = 0.85 \text{ Ref. a, b, c}$$

$$\frac{F(1,2)}{F(0,1)} = 1.78 \text{ Ref. a, b}$$

and for C_2

$$\frac{F(1,1)}{F(0,0)} = 0.464 \text{ Ref. a, b}$$

- (a) J. C. Burns, W.R.E. Adelaide (private correspondence).
- (b) Frazer, Jarman and Nichols, *Astrophysical Journal*, January 1954.
- (c) Leskov and Vasil'eva, transactions of the 11th All Union Conference on Theoretical Spectroscopy: Moscow 1957.

The value of $F(1,2)/F(0,1)$ for CN given by Leskov and Vasil'eva of 1.62 ± 0.02 has not been used in this work. If theoretical Top-Height Ratios are computed using this value, temperatures in excess of 7000°K are obtained from the measured band-head intensity ratios. Since the values of $F(1,2)/F(0,1)$ for CN given by Burns, and Frazer et al are mutually consistent and the measured temperatures using the average of their values (Section 2.3.2) are in reasonable agreement with temperatures deduced from the resolved rotation spectra (Section 2.3.1), the result of Leskov and Vasil'eva appears to be anomalous.

2

.

2

.

.

.

APPENDIX 3

CALCULATION OF PLASMA TEMPERATURE FROM MEASURED VALUES OF ELECTRON DENSITY

1 DETERMINATION OF ELECTRON DENSITY

The electron density of the plasma was evaluated from the distribution of intensity in the H β or H γ profile using the method described in detail in the paper by Fusey, Lapworth and Metherell¹⁴.

Briefly, this method involved normalizing the intensity distribution. Then the normalized distribution was multiplied by an appropriate factor, F_0 , so that the distribution fitted the theoretical distribution of the H β or H γ profile calculated by Griem, Kolb and Shen¹³. Theoretical and experimental intensity distributions for one of the better experimental H β profiles is shown in Fig. 8. The corresponding distributions for H γ are shown in Fig. 9.

According to the treatment given in Ref. 13 and 14 the electron density N_e is related to the scaling factor F_0 by equation 11.

$$F_0 = 2.61 e N_e^{2/3} \text{ (e. s. u.)} \quad (11)$$

2 DETERMINATION OF THE TEMPERATURE

The plasma is assumed to be an ideal conducting gas in thermal equilibrium at the equilibrium temperature, T,

The constituents of the plasma are assumed to be:-

N_e	electrons per cm ³
N_H	hydrogen atoms per cm ³
N_H^+	hydrogen ions per cm ³
N_O	oxygen atoms per cm ³
N_O^+	oxygen ions per cm ³
N_C	carbon atoms per cm ³
N_C^+	carbon ions per cm ³

Second ionization products have been neglected as second ionization potentials of oxygen and carbon are both large compared with their first ionization potentials

The equilibrium concentrations of atoms and ions of the constituent elements in the presence of the electrons at the equilibrium temperature, T, are given by the Saha equations for these elements.

Hydrogen

$$\frac{N_H^+ N_e}{N_H} = \psi_H \quad (12)$$

Oxygen

$$\frac{N_o^+ N_e}{N_o} = \psi_o \quad (13)$$

Carbon

$$\frac{N_C^+ N_e}{N_C} = \psi_C \quad (14)$$

In a general Saha function

$$\psi = \frac{2(2\pi m kT)^{3/2}}{h^3} \left(\frac{B^+}{B} \right) \exp - e \frac{(\chi - \Delta\chi)}{kT}$$

$\frac{2(2\pi m kT)^{3/2}}{h^3}$ is the partition function for the electrons.

m = electronic mass = 9.108×10^{-31} Kgm

k = Boltzmann's constant = 1.380×10^{-23} joule $^{\circ}K^{-1}$

h = Planck's constant = 6.625×10^{-34} joule-sec

B^+/B is the ratio of the partition functions of ions and atoms

χ is the ionization potential (eV)

e is the electronic charge 1.602×10^{-19} coul.

$\Delta\chi$ is the reduction of the ionization potential due to broadening of the bound energy states near the ionization level

$$\Delta\chi = 7.0 \times 10^{-7} N_e^{1/3} \text{ eV } (N_e \text{ in cm}^{-3})$$

The condition for charge neutrality is assumed to hold within the plasma and:-

$$N_H^+ + N_o^+ + N_C^+ = N_e \quad (15)$$

The plasma is assumed to be an ideal gas, the total pressure of which is comprised of the sum of the partial pressures of all the constituents. (Dalton's Law of Partial Pressures)

$$N_e + N_H^+ + N_H + N_O^+ + N_O + N_C^+ + N_C = p/kT \quad (16)$$

The effects of any de-mixing processes occurring in the plasma have been ignored and the proportions of hydrogen ions and atoms to oxygen ions and atoms are taken to be the same as for pure water.

Therefore

$$N_H^+ + N_H = 2(N_O^+ + N_O) \quad (17)$$

The evaporation of carbon into the water plasma occurs at a rate which could neither be measured nor deduced so the concentration of carbon ions and atoms is made the parameter of these equations.

Let there be x atoms of carbon for every atom of oxygen in the plasma. Then,

$$N_C^+ + N_C = x(N_O^+ + N_O) \quad (18)$$

Considering T as the dependent variable, the equations 12-18 contain eight independent variables, N_H , N_O , N_C , N_H^+ , N_O^+ , N_C^+ , x , N_e . N_C is obtained from measurements on $H\beta$ or $H\gamma$ profiles and x is the parameter of the equations.

Simultaneous solution of the seven equations 12-18 gives a result which can be reduced to the form:-

$$\frac{(3+x)N_e}{\left(\frac{P}{kT} - N_C\right)} = \frac{2}{\left(\frac{N_e}{\psi_H} + 1\right)} + \frac{1}{\frac{N_e}{\psi_O} + 1} + \frac{x}{\frac{N_e}{\psi_C} + 1} \quad (19)$$

When the case of the pure water plasma is considered, $x = 0$, and equation 19 is identical to the equation (4.3.10) deduced by Pusey, Lapworth and Metherell¹⁴ for the relationship between N_e and temperature.

The ratio of statistical weights for a temperature of 10,000°K and ionization potentials taken from "Astrophysical Quantities" by C.W. Allen¹² were as follows:-

	B^+/B	(eV)
Hydrogen	0.5	13.595
Oxygen	0.447	13.614
Carbon	0.602	11.256

Substituting these numerical values in equations 12, 13, 14 we get.-

$$\psi_H = 2.415 \times 10^{15} T^{3/2} \exp - \frac{(157810 - 0.008124 N_e^{1/3})}{T} \quad (20)$$

$$\psi_O = 2.159 \times 10^{15} T^{3/2} \exp - \frac{(158040 - 0.008124 N_e^{1/3})}{T} \quad (21)$$

$$\psi_C = 2.908 \times 10^{15} T^{3/2} \exp - \frac{(130670 - 0.008124 N_e^{1/3})}{T} \quad (22)$$

The measured value of electron density taken was $3.42 \times 10^{16} \text{ cm}^{-3}$ from Section 3.3.2, and equation 19 has been solved graphically for T using values for x of 0, 0.1, 0.25, 0.5, 0.75, 1.0. The solutions for T are given in Fig. 10.

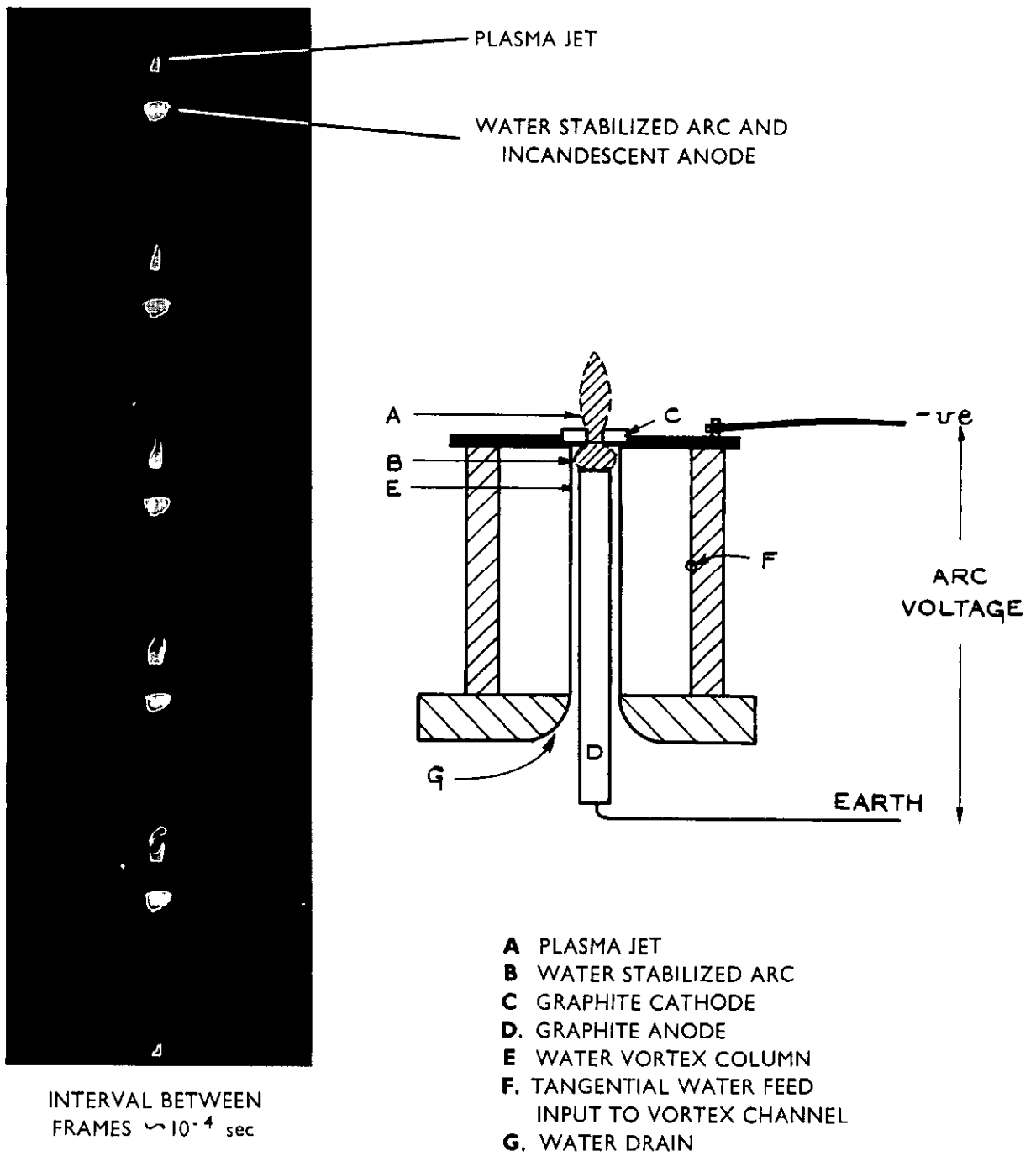


FIG.1. PLASMA JET APPARATUS TOGETHER WITH A HIGH-SPEED CINE FILM RECORD OF PLASMA JET

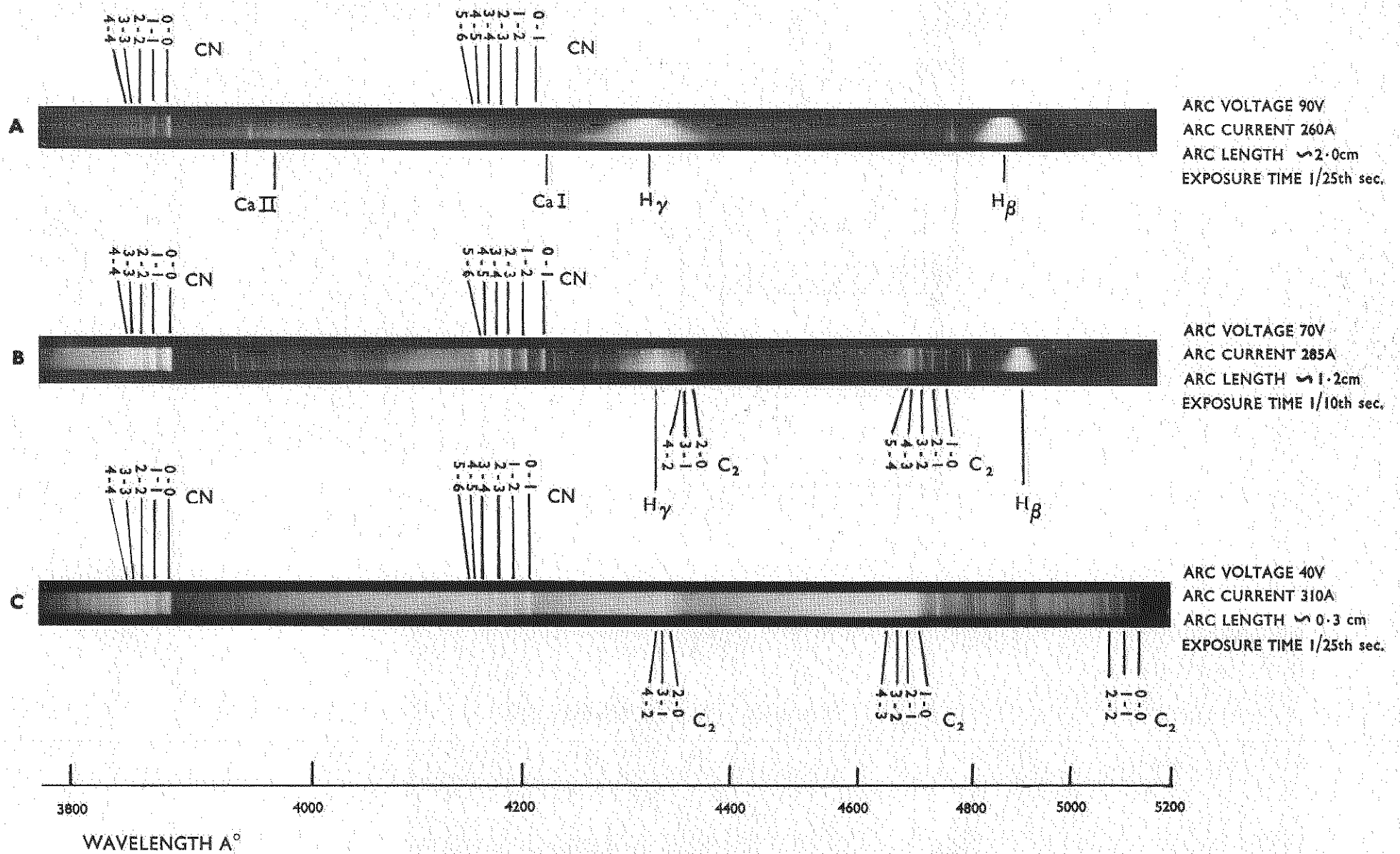


FIG.2. JET SPECTRUM FOR A RANGE OF ARC CONDITIONS

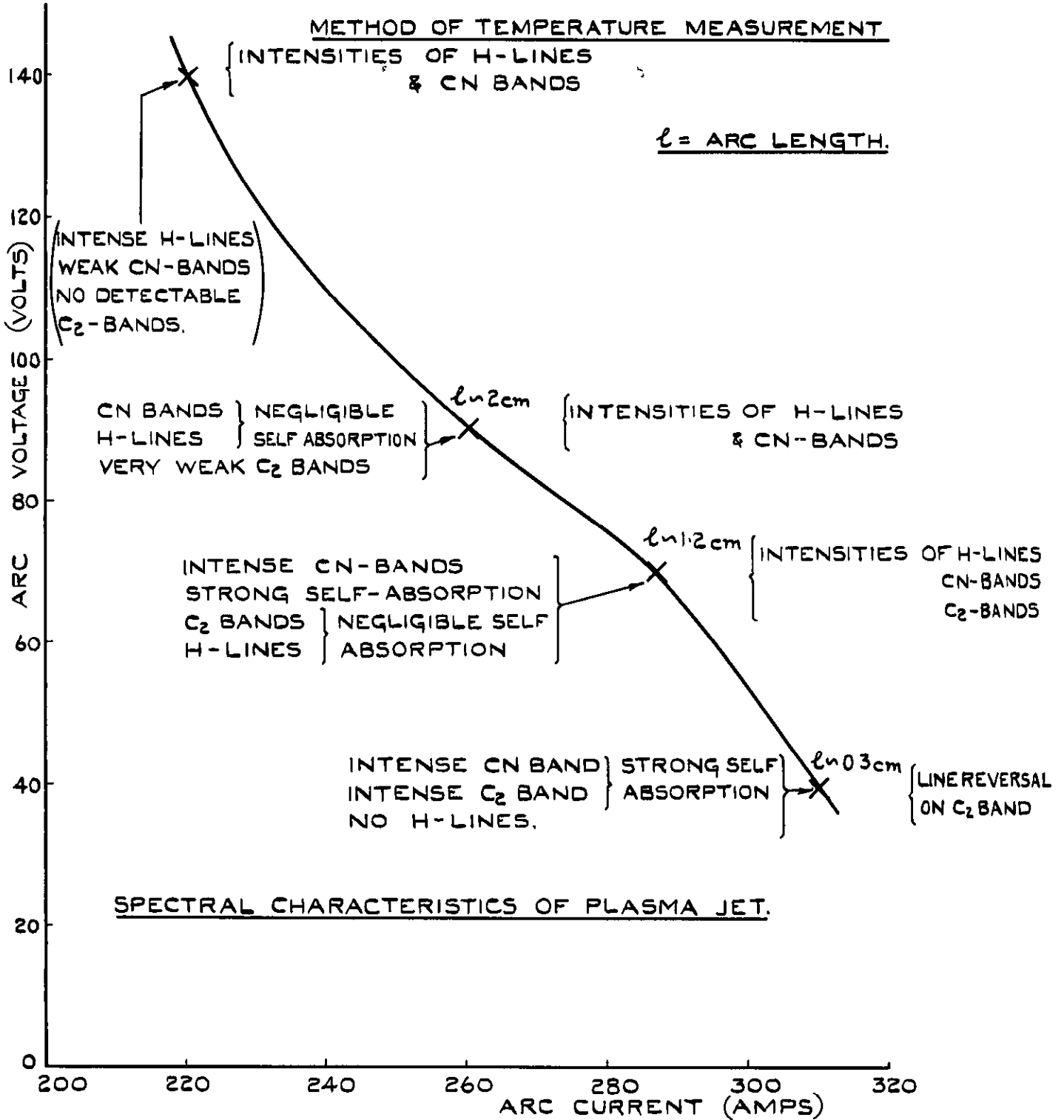


FIG.3. INTERDEPENDENCE OF SPECTRAL CHARACTERISTICS OF PLASMA JET ON THE ARC VOLTAGE, CURRENT AND LENGTH.

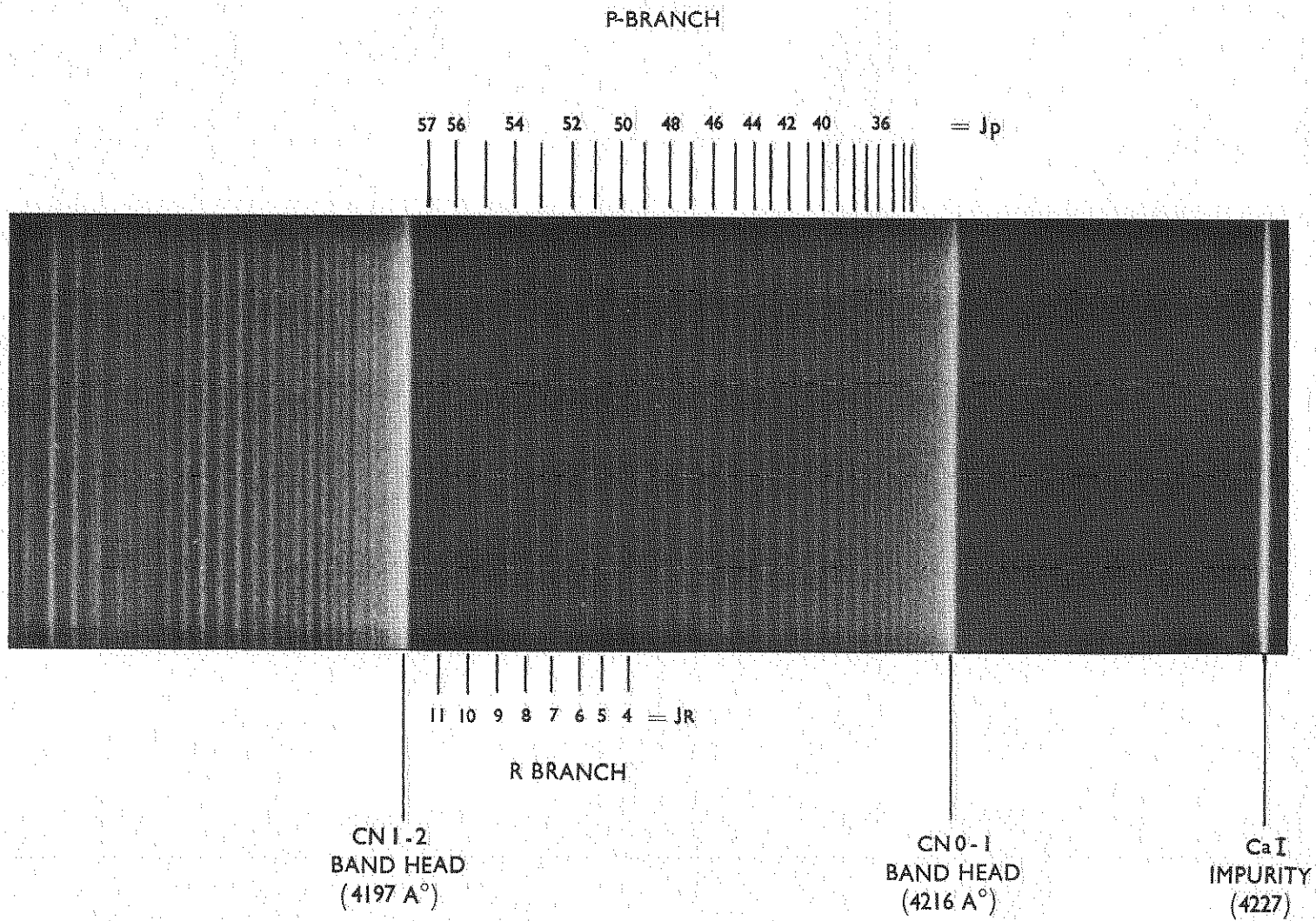
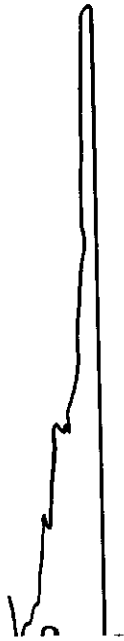


FIG.4A. SPECTROGRAM OF RESOLVED $B^2\Sigma^+ - X^2\Sigma^+$ CN 0-1 (AND CN 1-2) BANDS

DENSITY (ARB. UNITS)



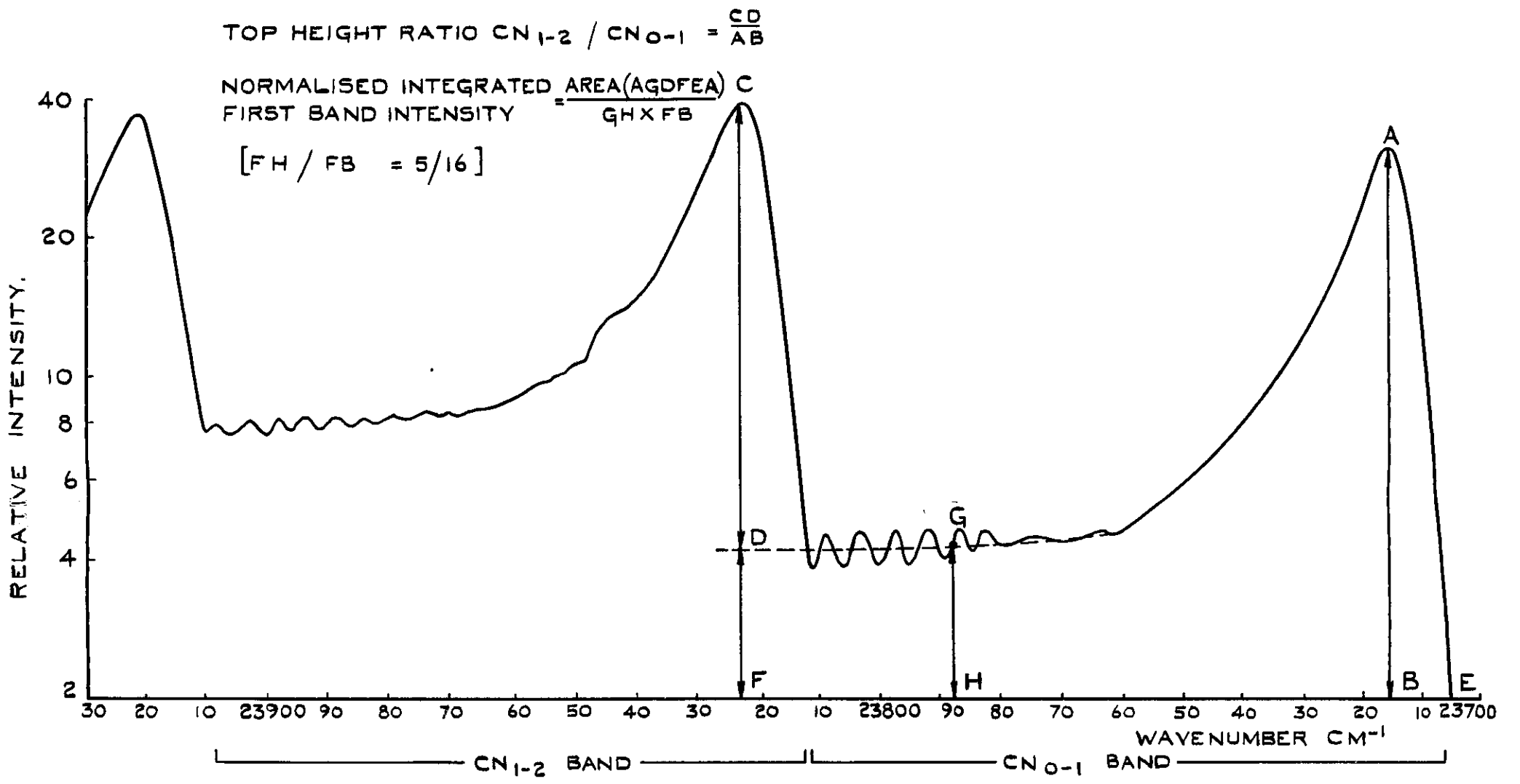
SPECTRUM DETAILS.-

30,000 LINES PER INCH PLANE GRATING LITTROW SPECTROGRAPH
15 μ SLIT, 4 SEC EXPOSURE, 5 \AA /m.m. DISPERSION

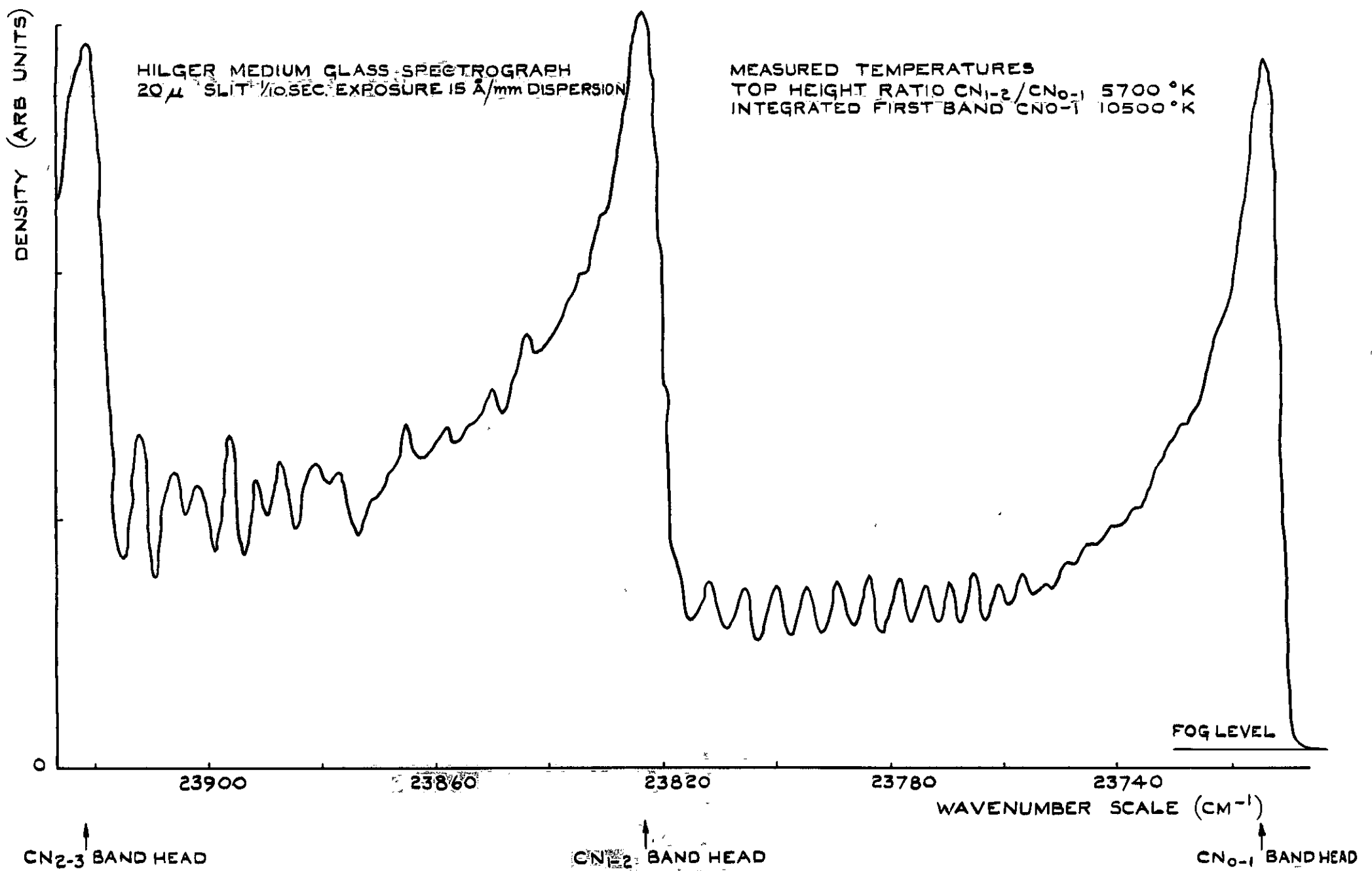
MICRODENSITOMETER DETAILS: MAGNIFICATION OF
WAVELENGTH SCALE 50:1 DENSITY RANGE 0-20.

INTERSECTION WAVE NUMBER = 23821.2 cm^{-1}
TEMPERATURE = 5820 $^{\circ}\text{K}$





(a) THEORETICAL UNRESOLVED $CN_{0,1}$ AND $1,2$ BANDS. (TEMP=6000 °K, $b=8 cm^{-1}$)



(b) MICRODENSITOMETER TRACE OF UNRESOLVED CN_{0-1} AND CN_{1-2} BANDS.

FIG. 5. THEORETICAL AND EXPERIMENTAL CN_{0-1} AND CN_{1-2} BAND PROFILES

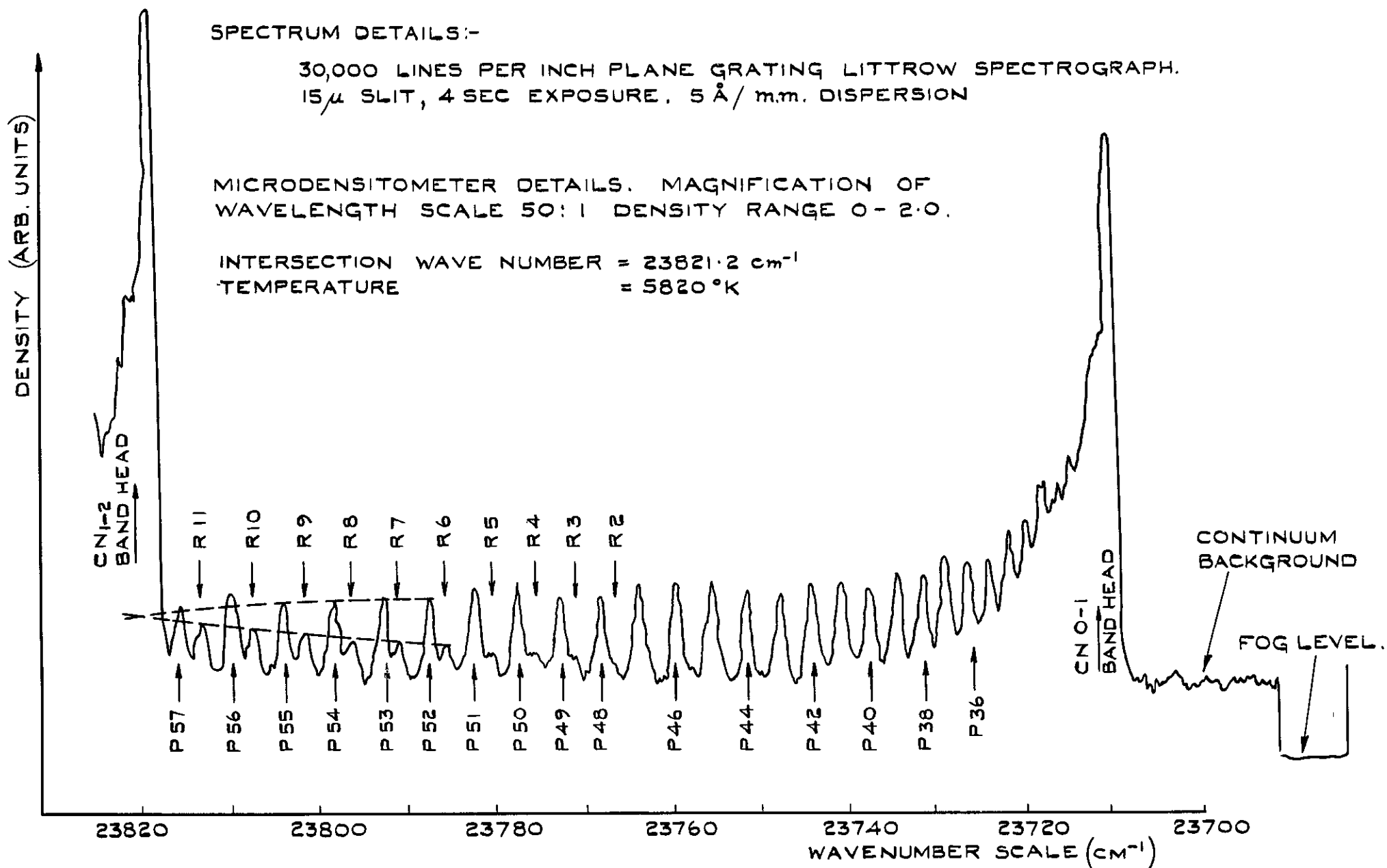


FIG.4 (b) MICRODENSITOMETER RECORD OF CN O-1 BAND.

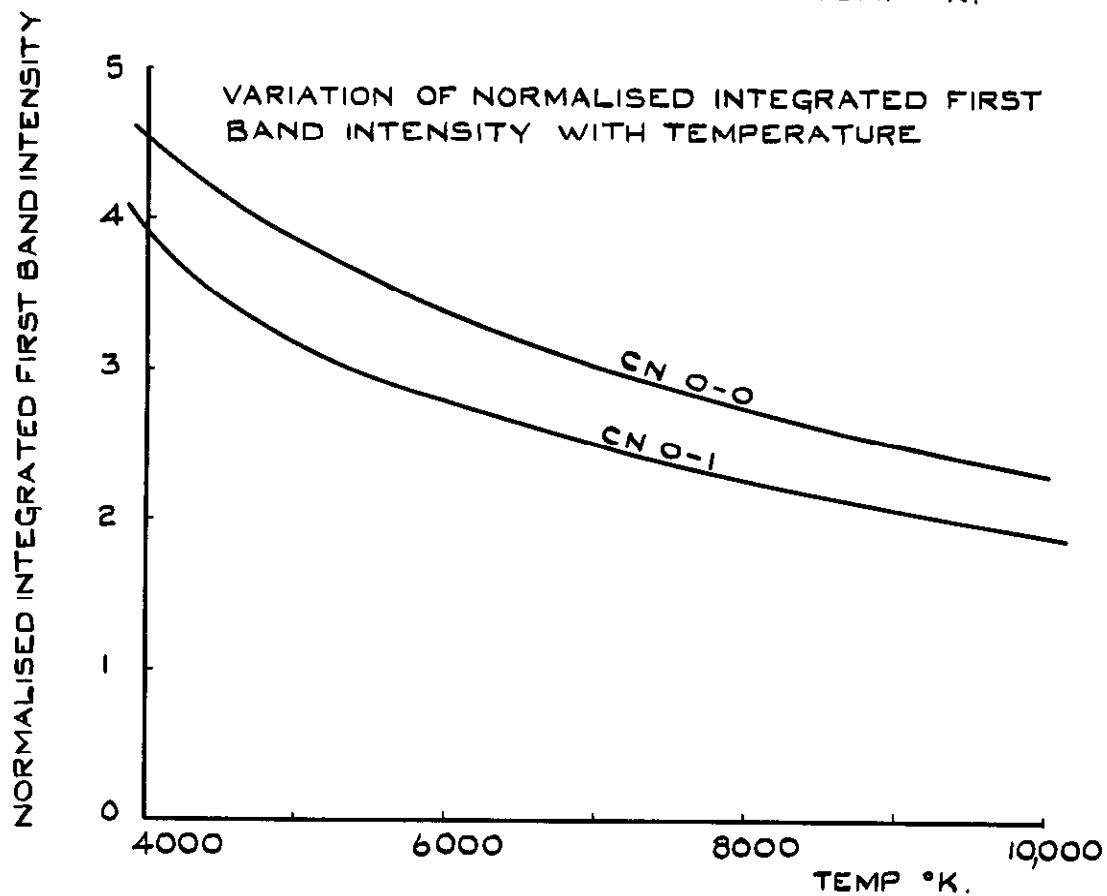
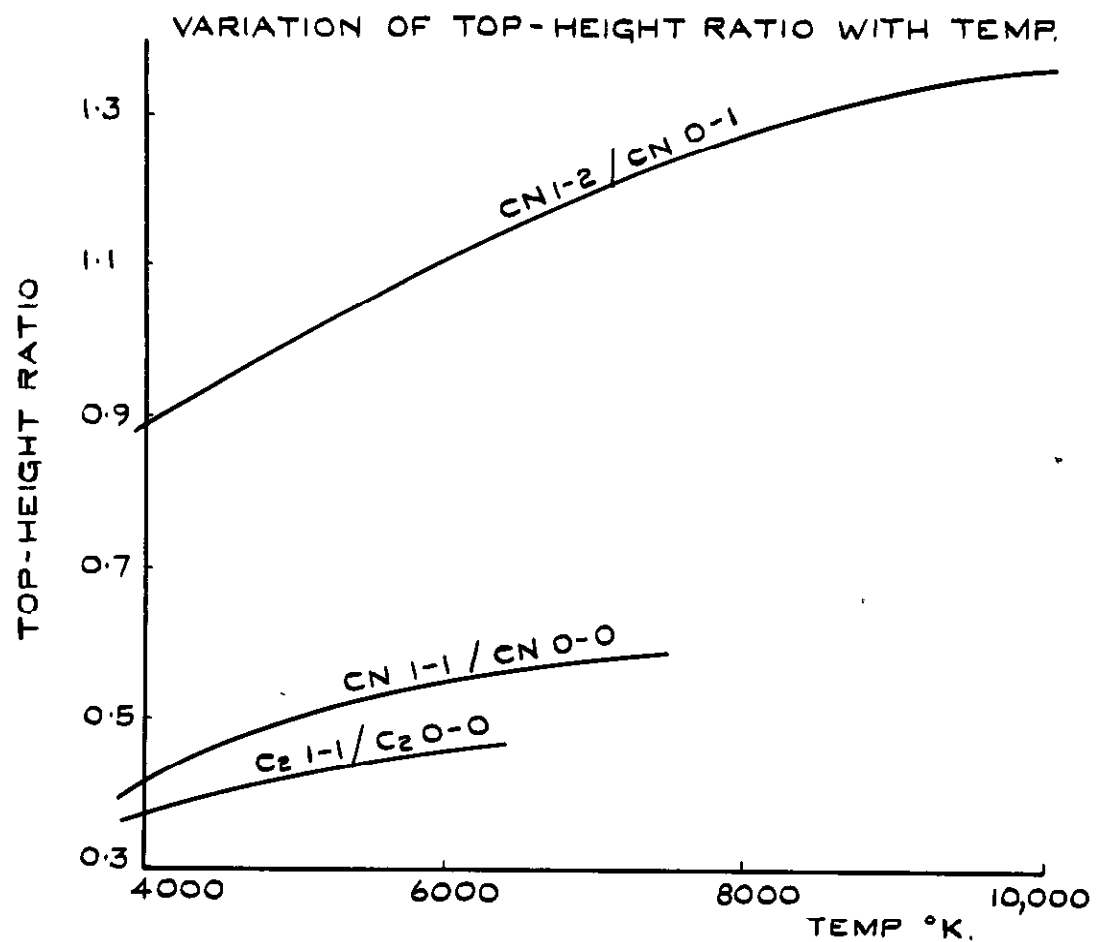


FIG.6. DEPENDENCE ON TEMPERATURE OF TOP-HEIGHT INTENSITY RATIO AND INTEGRATED FIRST BAND INTENSITIES.

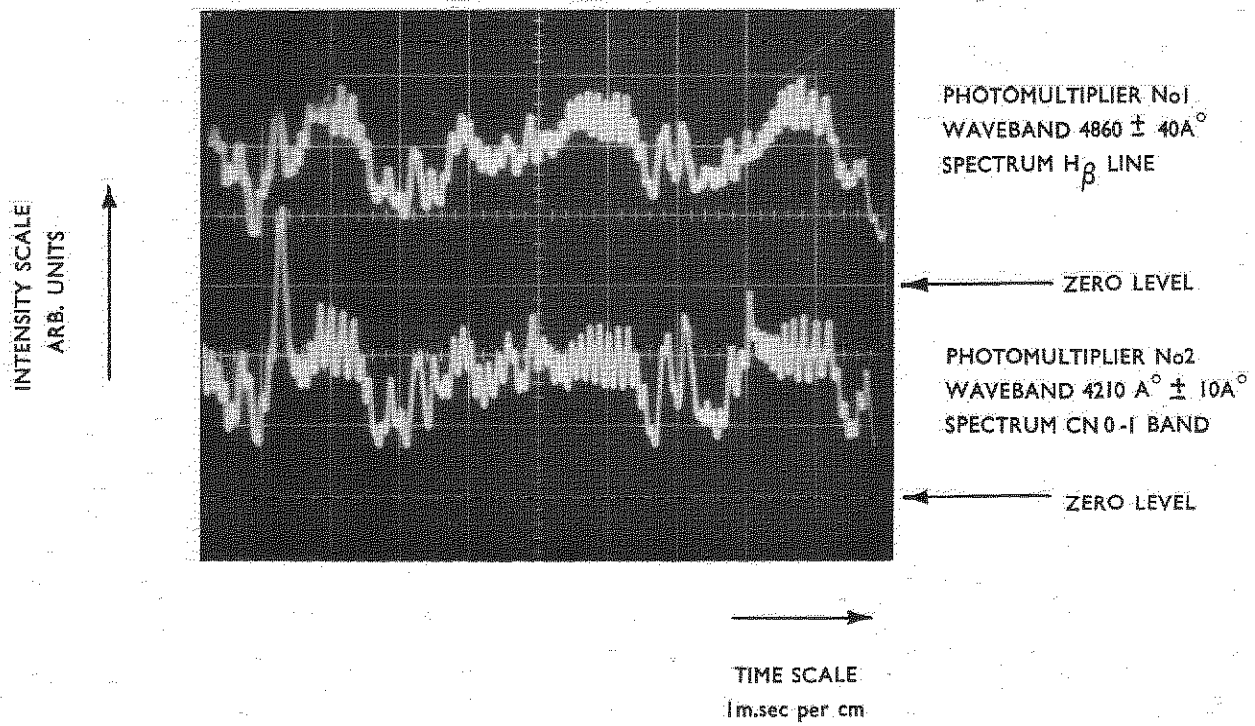


FIG.7. TIME-RESOLVED INTENSITY VARIATIONS
IN THE PLASMA JET

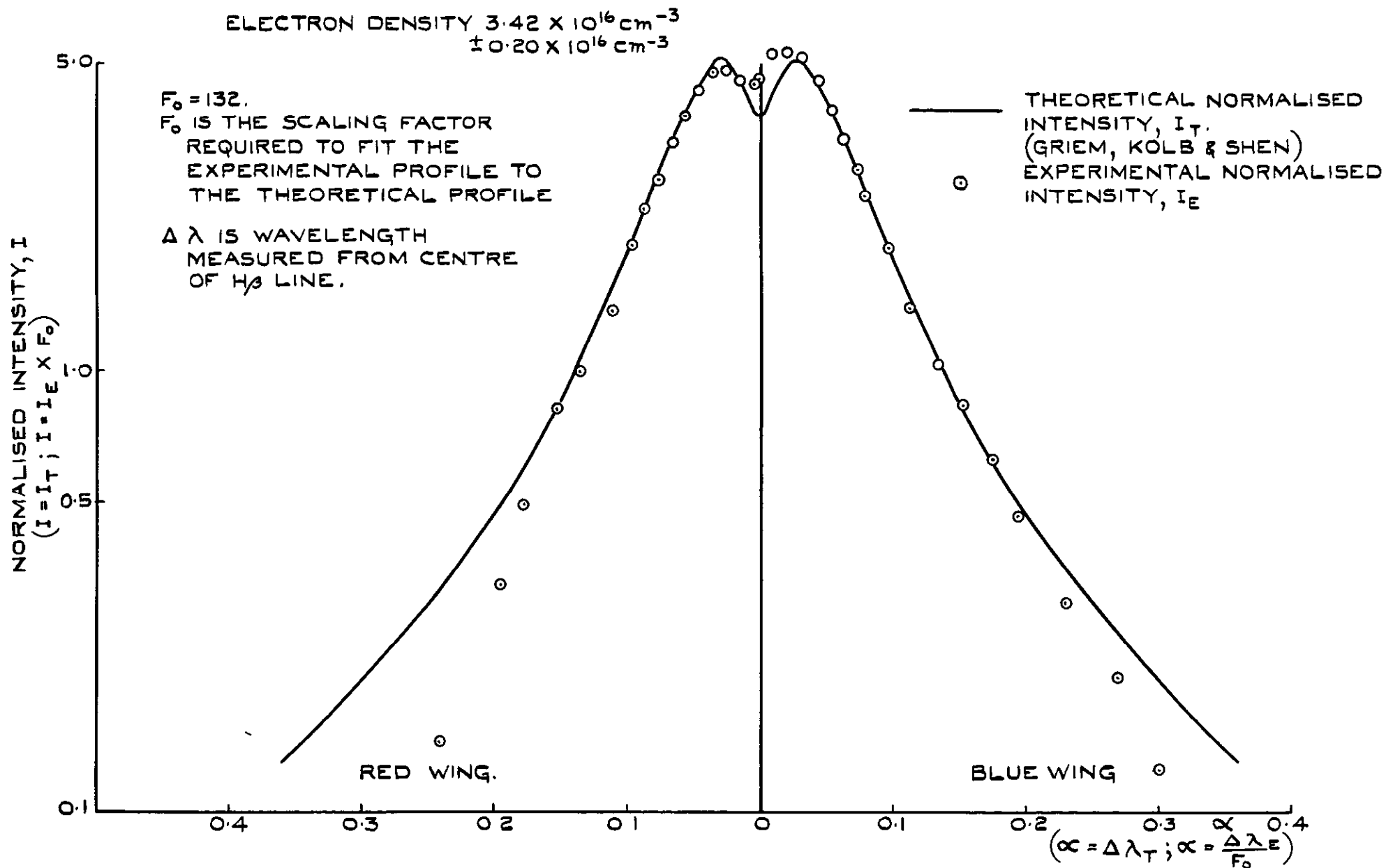


FIG. 8. THEORETICAL & EXPERIMENTAL INTENSITY
 DISTRIBUTIONS IN THE H_{β} LINE (4861 \AA) OF HYDROGEN.

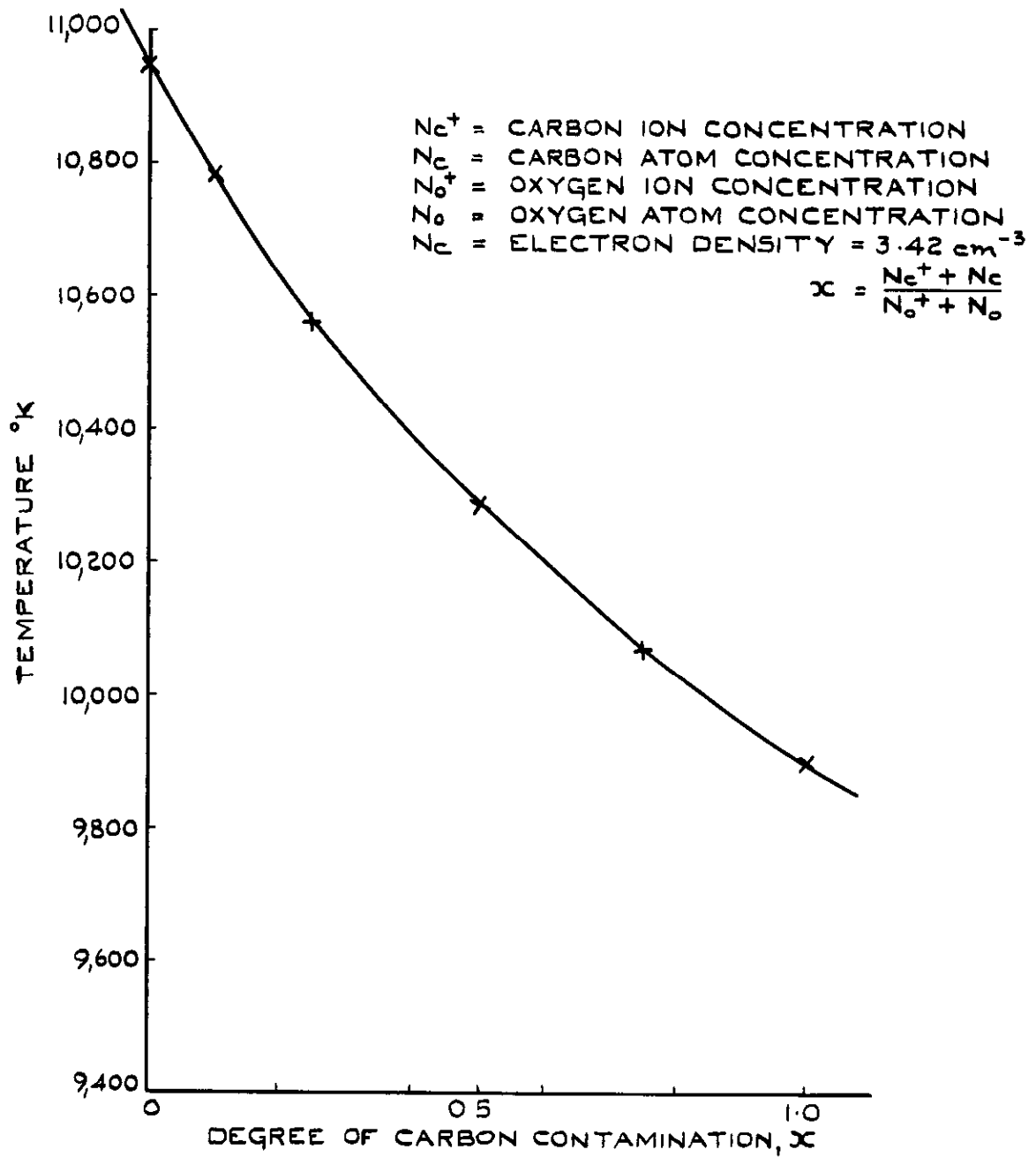


FIG. 10. THEORETICAL DEPENDENCE OF WATER PLASMA TEMPERATURE ON CONTAMINATION WITH CARBON.

3

•

•

•

•

•

A.R.C. C.P. No.756

538.3:
532.5:
536.52:
535.33

TEMPERATURE MEASUREMENTS ON A PLASMA JET. Wells, A. and Kennett, R.H. February 1964.

Temperature measurements have been performed using spectroscopic techniques on the plasma jet obtained from a water stabilized arc with carbon electrodes.

The jet spectrum in the visible region consisted primarily of band spectra of molecular CN and C₂ and the Stark-broadened atomic line spectra of hydrogen. Intensities in various parts of these spectra were measured and temperatures were then deduced

(a) from unresolved rotation line intensities in the CN 0-1 band,

(Over)

A.R.C. C.P. No.756

538.3:
532.5:
536.52:
535.33

TEMPERATURE MEASUREMENTS ON A PLASMA JET. Wells, A. and Kennett, R.H. February 1964.

Temperature measurements have been performed using spectroscopic techniques on the plasma jet obtained from a water stabilized arc with carbon electrodes.

The jet spectrum in the visible region consisted primarily of band spectra of molecular CN and C₂ and the Stark-broadened atomic line spectra of hydrogen. Intensities in various parts of these spectra were measured and temperatures were then deduced

(a) from unresolved rotation line intensities in the CN 0-1 band,

(Over)

A.R.C. C.P. No.756

538.3:
532.5:
536.52:
535.33

TEMPERATURE MEASUREMENTS ON A PLASMA JET. Wells, A. and Kennett, R.H. February 1964.

Temperature measurements have been performed using spectroscopic techniques on the plasma jet obtained from a water stabilized arc with carbon electrodes.

The jet spectrum in the visible region consisted primarily of band spectra of molecular CN and C₂ and the Stark-broadened atomic line spectra of hydrogen. Intensities in various parts of these spectra were measured and temperatures were then deduced

(a) from unresolved rotation line intensities in the CN 0-1 band,

(Over)

- (b) from unresolved band intensities in the CN and C₂ systems,
- (c) from total intensities in the hydrogen H β and H γ lines,
- (d) from the Stark-broadened line profiles of the H β and H γ lines.

Temperatures were also measured by the method of spectrum-line reversal on the C₂ 1-0 band head.

Temperatures obtained simultaneously from measurements on the CN band systems and the H β line profiles differed considerably; an average temperature of 5800°K \pm 300°K was obtained from measurements on the CN band spectrum whilst a temperature of 10,960°K \pm 400°K was obtained from the H β profile. This apparent inconsistency has been attributed to the existence of zones at different temperatures in the jet structure.

Observed jet instabilities have been reported and discussed and the limitations of the experimental techniques have also been commented upon.

- (b) from unresolved band intensities in the CN and C₂ systems,
- (c) from total intensities in the hydrogen H β and H γ lines,
- (d) from the Stark-broadened line profiles of the H β and H γ lines.

Temperatures were also measured by the method of spectrum-line reversal on the C₂ 1-0 band head.

Temperatures obtained simultaneously from measurements on the CN band systems and the H β line profiles differed considerably; an average temperature of 5800°K \pm 300°K was obtained from measurements on the CN band spectrum whilst a temperature of 10,960°K \pm 400°K was obtained from the H β profile. This apparent inconsistency has been attributed to the existence of zones at different temperatures in the jet structure.

Observed jet instabilities have been reported and discussed and the limitations of the experimental techniques have also been commented upon.

- (b) from unresolved band intensities in the CN and C₂ systems,
- (c) from total intensities in the hydrogen H β and H γ lines,
- (d) from the Stark-broadened line profiles of the H β and H γ lines.

Temperatures were also measured by the method of spectrum-line reversal on the C₂ 1-0 band head.

Temperatures obtained simultaneously from measurements on the CN band systems and the H β line profiles differed considerably; an average temperature of 5800°K \pm 300°K was obtained from measurements on the CN band spectrum whilst a temperature of 10,960°K \pm 400°K was obtained from the H β profile. This apparent inconsistency has been attributed to the existence of zones at different temperatures in the jet structure.

Observed jet instabilities have been reported and discussed and the limitations of the experimental techniques have also been commented upon.

C.P. No. 756

© *Crown Copyright 1964*

Published by
HER MAJESTY'S STATIONERY OFFICE

To be purchased from
York House, Kingsway, London w.c.2
423 Oxford Street, London w.1
13A Castle Street, Edinburgh 2
109 St. Mary Street, Cardiff
39 King Street, Manchester 2
50 Fairfax Street, Bristol 1
35 Smallbrook, Ringway, Birmingham 5
80 Chichester Street, Belfast 1
or through any bookseller

C.P. No. 756

S.O. CODE No. 23-9015-56